Principles of Ageing of Double Base Propellants and its Assessment by Several Methods Following Propellant Properties

Manfred A. Bohn
Fraunhofer Institute of Chemical Institute (ICT)
D-76318 Pfinztal-Berghausen
GERMANY

Manfred.Bohn@ict.fraunhofer.de

ABSTRACT

Nitrocellulose (NC) based double base (db) rocket propellants (RP) are further on in use because of adaptable properties in burning rate and the low signature. The slow ageing during storage is often seen as a major disadvantage. However, this is not the case in reality. If properly manufactured with carefully selected ingredients, in-service times up to 20 years at normal thermal loads (10 to 30°C) can be obtained easily. To secure the in-service time handling of db RP motors, one should use the proven ageing indicators: decrease of primary (added at manufacture) stabilizer, decrease of molar mass of NC, heat generation rate determined by heat flow microcalorimetry (HFMC). They are used to determine the state of chemical ageing and to predict residual in-service time. Further ageing indicators are tensile strength at break, mass loss and gas generation. DMA (dynamic mechanical analysis) can answer special questions. On the base of these methods, the adapted concept for the health monitoring of db RP can be established and implemented.

To assess the chemical ageing of db RP, first the principle decomposition mechanisms are outlined. The concept of different activation energies is explained and rationalised by newer investigation results. The decomposition ways with different activation energies can influence significantly the prediction and assessment of remaining in-service time. After the selection of ageing indicators, the description of the change of measured data with time must be achieved. This paper shows the principles and ways to predict residual in-service time using stabilizer decrease and molar mass decrease, as well as heat generation rate and tensile strength. For this, the kinetic description models are presented and evaluated as well as simplified methods used to predict a limited in-service time interval. Mass loss as stability indicator is discussed also. A property often somewhat neglected is gas generation. An important assessment example is outlined. Further, an example with DMA is presented. Finally, some remarks on the evaluation of so-called 'green' stabilizers should help to get suitable assessment of them. A compilation of test and investigation methods for db RP can be found also. As a whole, the complexity of ageing mechanism seems higher with db RP than with typical HTPB-based composite RP.

Keywords
Double base propellants, chemical stability, in-service time predictions, stabilizer decrease, molar mass degradation, heat generation rate, DMA, gas generation

1.0 INTRODUCTION

Double base rocket propellants fulfil an important part in propelled devices: tactical rockets, anti-structure weapons, emergency eject systems, small artillery weapons and others. A db RP is used, when minimum signature is demanded up to medium performance level. Mostly they are homogenous in contrast to composite propellants based on rubbery binder and AP (ammonium perchlorate) and AL (aluminium

powder). Typically they consist of two main components: nitrocellulose (NC) (N content around 12.6 mass-%), and a nitrate ester plasticizer, often nitroglycerine (NG). Further needed is a stabilizer as 2-nitro-diphenylamine (2-NO_2-DPA) or ethyl centralite (EC, centralite I), or akardite II. The diphenylamine (DPA) is also an effective stabilizer but not used in double base propellants, because it reacts to fast with NG. All these stabilizers have so-called activated phenyl rings as the reactive molecular sites to catch NO_2. The reaction between NO_2 and the stabilizers is of type radical substitution. Burning catalysts are added to achieve plateau burning, which increases burning stability. Such substances can be lead(II) salicylate and copper(II) resorcylate. Plasticizers can be ethylphenylurethane, dioctyl phthalate, dioctyl adipate and others.

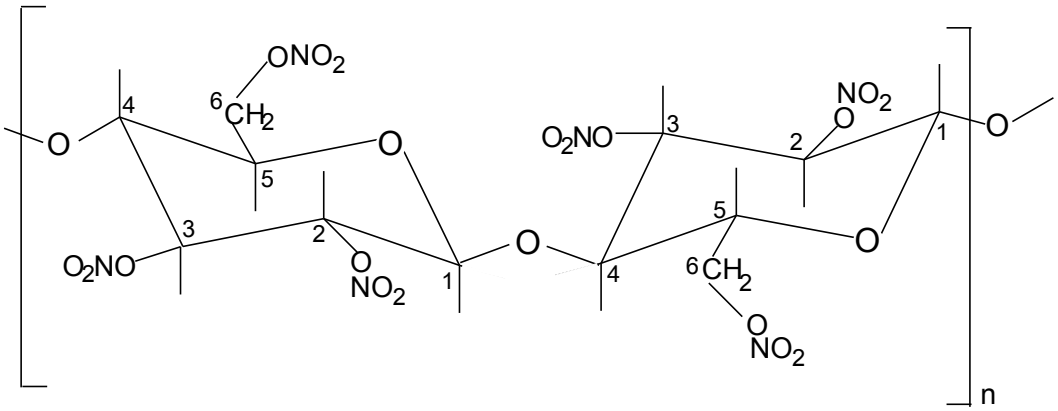

Figure 20-1: Monomer base of nitrocellulose, shown is as example the formally fully nitrated monomer. The nitration occurs at the ring positions C2 and C3 and at the CH2 group at position 5, named C6. The monomeric unit is the one of cellobiose. The connection between two glucosidic units is called: 1→4-O-β-D-glucosidic bond or (generally) 1→4-O-β-D-glycosidic bond. The β means bonding via equatorial orientation; α means bonding via axial orientation.

Nitrate esters (NE) as NC decompose slowly and split-off NOx, which accelerate the decomposition. Therefore, the split-off NOx (named as P in the reaction scheme) must be 'neutralized' by bonding to stabilizers (S), which supresses the autocatalytic decomposition cycle. But one has to keep in mind that the intrinsic decomposition cannot be prevented and the decomposition is always going on but without running away as long as active stabilizer is present. Ideally, the second reaction scheme is established, without autocatalysis.

$$NE \xrightarrow{k_{NE}} P + R \qquad \text{intrinsic decomposition}$$
$$NE + P \xrightarrow{k_{auto}} 2\,P + R \qquad \text{autocatalytic decomposition}$$
$$S + P \xrightarrow{k_S} P\text{-}S \qquad \text{stabilising reaction}$$

$$NE \xrightarrow{k_{NE}} P + R \qquad \text{intrinsic decomposition}$$
$$S + P \xrightarrow{k_S} P\text{-}S \qquad \text{stabilising reaction}$$

A further complication arises from two interfering substances: oxygen and water. Oxygen as biradical, $^{\bullet}O{=}O^{\bullet}$, is involved in the radically reactions of $^{\bullet}NO_2$ and $^{\bullet}NO$, both also radicals, means they have one unpaired valence electron each. Oxygen easily oxidises $^{\bullet}NO$ to $^{\bullet}NO_2$, which is much more aggressive in the material. The intermediate formation of the 'peroxide' $^{\bullet}OO\text{-}NO$ serves also as very reactive species. Radical chain reactions based on $^{\bullet}OH$ and $^{\bullet}OOH$ radicals can occur in principle. Water has two effects: it

fosters hydrolytic splitting of the nitrate ester groups and of the NC chain at the 1,4-β-glucosidic coupling between the glucose rings. NO_2 and water can form nitric and nitrous acid, again fostering hydrolytic splitting. $^{\bullet}NO_2$ may react also from its condensed form $_2ON\text{-}NO_2$ (this has a very low bond dissociation enthalpy of about 57 kJ/mol), which facilitates the radicalic substitution on the phenyl rings of the stabilizers. The next complication arises from the fact that the three possible nitrate ester positions on a glucosidic ring, named better anhydroglucopyranose (AHP) ring, of the basic NC unit have different bond dissociation energies and bond dissociation enthalpies in the $CO\text{-}NO_2$ bonds [1].This is discussed in more detail in the next section.

2.0 SOME DETAILS ON NC DECOMPOSITION

As said above we have at least three mechanistic decomposition ways with NC: (1) thermolytic cleavage of $CO\text{-}NO_2$ bond, producing $CO^{\bullet}$ and $^{\bullet}NO_2$ radicals; (2) hydrolytic cleavage of $CO\text{-}NO_2$ bond; (3) hydrolytic cleavage of the 1,4-β-glucosidic bond. Important to note is the following: By thermolytically splitting of the NE group ($CO\text{-}NO_2$) on the glucosidic NC ring a radical functionality is formed at the ring. By stabilisation reactions, mostly this ring is destroyed and the NC chain is split. This means, in spite of the presence of active stabilizer, we have the intrinsic decomposition of NE groups and in connection therewith a NC chain degradation. This situation increases further in complexity in that these different decomposition ways have different activation energies and therefore the temperature dependence of these three reaction ways is different, as shown in Fig. 2. The reaction rate constant of ET (ester thermolysis) is at low temperatures, 30°C, much lower than the one of ester hydrolysis (EH); but this is reversed at higher temperatures, see 90°C. It depends on the measurement type, what is seen. With stabilizer consumption one can recognize indirectly ET and EH. With molar mass degradation of NC, the mechanisms seen are ET and CH. With heat generation rate, this behaviour has not really been revealed, because one sees a global exothermal effect (NC decomposition, stabilizer reactions) and not a specific property alone, as stabilizer decrease and chain splitting of NC.

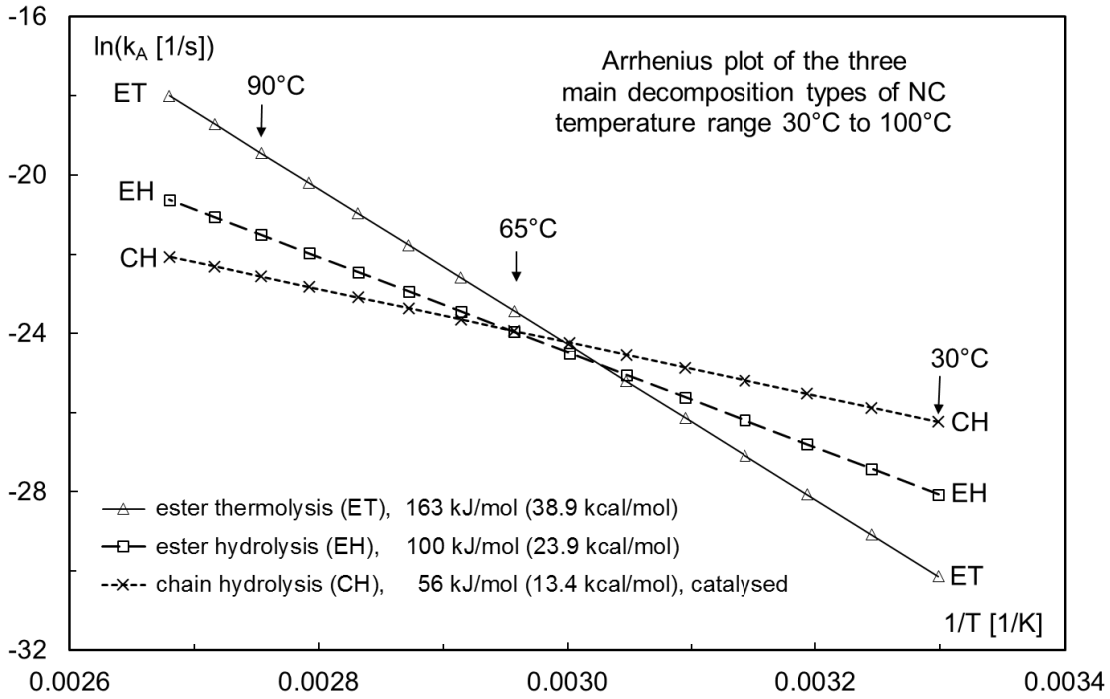

Figure 20-2: The interplay of the three main decomposition mechanisms governed by the different activation energies of the three reaction ways.

The Figure 3 shows the course of the reaction rate constants in the transition region, a real sharp bend cannot appear this is chosen only for clarification in the graphs. Experimental examples of such bends are shown in Fig. 4 and Fig. 5, with stabilizer decrease and mean molar mass Mw decrease in single base propellant A5020. Fig. 4 shows an example the overlay of thermolytical and hydrolytical NE decomposition, monitored indirectly via the rate of stabilizer consumption. Between 60°C and 90°C an activation energy of 146 kJ/mol is obtained, below 60°C only 86 kJ/mol occur. In Fig. 5 the situation for the decrease of mean molar mass Mw of the NC of A5020 is shown. Here also a bend occurs around 60°C. Above the same activation energy value was found as with stabilizer decrease, indication that at these higher temperatures mainly NC chain splitting according to thermolytical NE decomposition occurs with subsequent destruction of a glucosidic NC ring. Below 60°C a quite low activation energy is found corresponding to chain scission via hydrolytic cleavage of the 1,4-β-glucosidic bond. In addition, one must note that decrease of stabilizer consumption and decrease of mean molar mass of NC chains go in parallel. These data are published already [2].

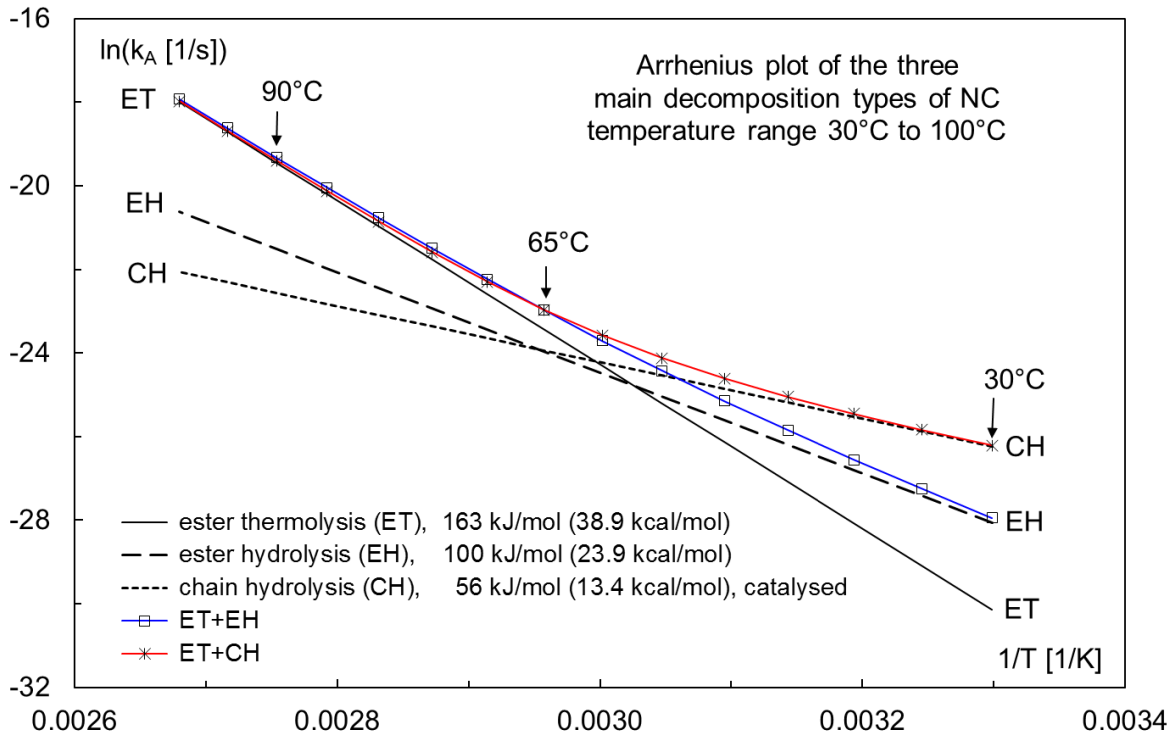

Figure 20-3: The combination of two mechanisms can be recognized via stabilizer consumption for ET and EH and via molar mass degradation for ET and CH. This means these two measurement quantities may show a bend in the Arrhenius plot of the corresponding reaction rate constants, means for stabilizer decrease (ET+EH) and for molar mass decrease (ET+CH).

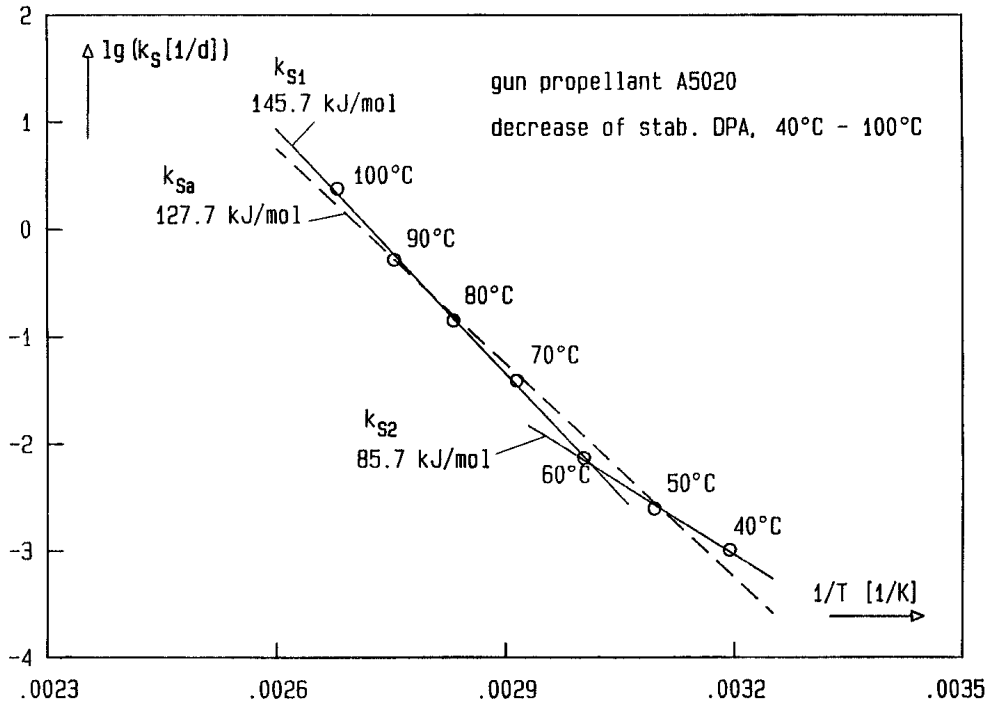

Figure 20-4: Example of a bend in Arrhenius plot of the reaction rate constant (first order model was used) for the DPA stabilizer decrease in single base gun propellant A5020. The higher temperature mechanism shows an activation energy of 146 kJ/mol, the lower temperature mechanism (below 60°C) has 86 kJ/mol.

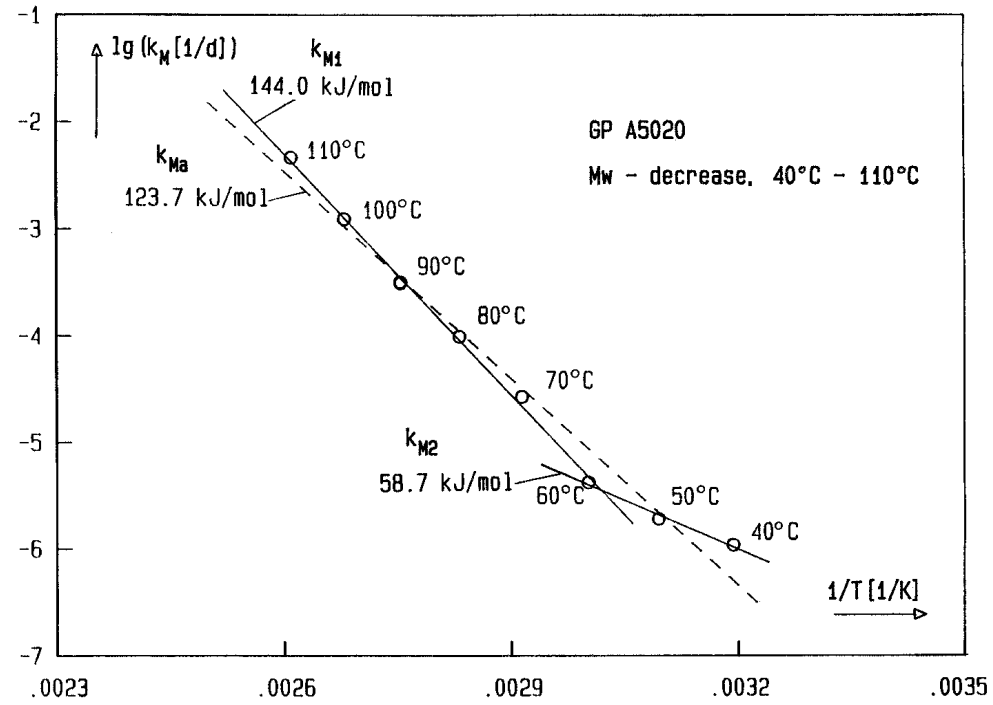

Figure 20-5: Example of a bend in Arrhenius plot of the reaction rate constant (random chain scission model was used) for the decrease of mean molar mass Mw of the NC in single base gun propellant A5020. The higher temperature mechanism shows an activation energy of 144 kJ/mol, the lower temperature mechanism (below 60°C) has 59 kJ/mol.

The problem with the different reaction rate constants along the temperature is even more complex. The three position have (1) quite different bond dissociation enthalpies and (2) the saponification rate is also different. In a special investigation of the decomposition of a nitrocellulose with N-content = 12.15 mass.%, see Table 1, the nitration of an aromatic dye was performed [3,4]. Thereby a stepwise nitration occurred. This is interpreted as caused by the three different NE-groups at the AHP rings, because of their different reactivity. The reaction of stabilizer with NO or NO_2 is of second order. During the initial period of decomposition, the approximation of first order for the stabilizer decrease is possible, assuming a constant concentration of the nitration species. The different partial degrees of substitution at the three sites are considered by the modelling. The modelling used all data at all temperatures at once and provided directly with the Arrhenius parameters and the weighting factors, which corresponds to the partial nitration at the three sites of the AHP ring.

Table 20-1: Characterising data of used NC to reveal the different reaction steps caused by the different reactivity of the NE-groups of NC

Property	**unit**	**value**
Nitrogen content	mass-%	12.15
Mean molar mass of one anhydroglucopyranose unit	g/mol	265.95
Mean total degree of substitution (TDS)	-	2.307
Content of ONO_2 groups	mass-%	53.79
Content of NO_2 groups	mass-%	39.91
Oxygen balance	%	-37.49

It is plausible that the split-off of NO_2 from a nitrate ester group occurs according to a reaction of first order. However, the active species in nitration may result from NO_2 radicals combining to give dinitrogentetroxide, N_2O_4. This would then lead to a reaction of second order with respect to stabilizer nitration reaction. In order to fulfil the radical neutrality, two radicals must be always involved in aromatic radically nitration, also in case of N-NO formation. Assuming N_2O_4 as active species, the corresponding rate equation for stabilizer consumption is Eq.(1). The [P(t)·P(t)] is seen as one species.

$$\frac{dS(t)}{dt} = -k'_F \cdot S(t) \cdot [P(t) \cdot P(t)] \qquad (1)$$

How to imagine the molecular processes: One split-off NO_2 snoops around. It still can recombine at the split-off site at the AHP ring. Accidentally it encounters a second one and forms N_2O_4, which is radically neutral. The second NO_2 may come from the same AHP ring or a neighbouring one. By forming N_2O_4 both NO_2 are lost for the NC, which has now formally degraded by second order. N_2O_4 is the attacking species in the stabilizer reaction, which is formally still bimolecular, because the two NO_2 radicals are spatially coordinated. The three parallel reaction of second order are normalized and the equation used to model the data is given in Eq.(2). The modelling of the data is shown in Figure 6. The data are compiled in Table 2 [4].

$$\frac{c_S(t,T)}{c_S(0)} = Sr(t,T) = A_2/(1+k_2(T)\cdot t) + A_3/(1+k_3(T)\cdot t) + A_6/(1+k_6(T)\cdot t) \qquad (2)$$

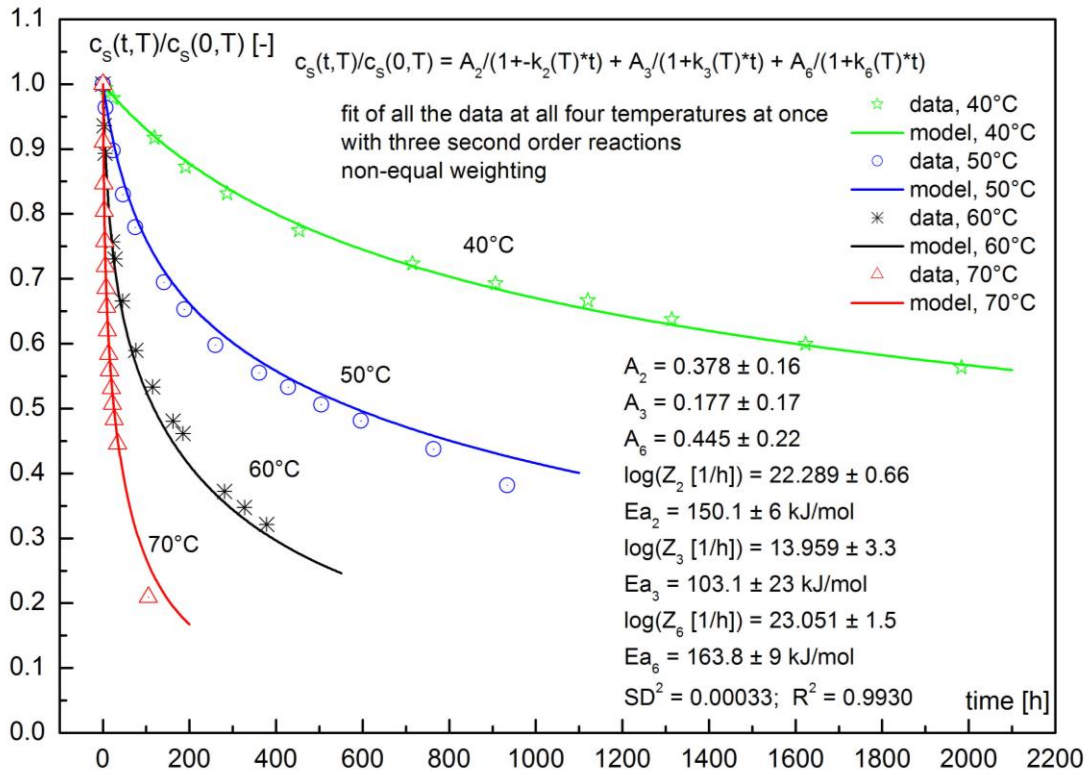

Figure 20-6: Modelling of the concentration courses of the aromatic dye with three reactions of second order occurring in parallel. Followed is un-nitrated dye concentration.

Table 20-2: Compilation of the results of the modelling. Interesting to note that the average value of the activation energy is with 148 kJ/mol in the very range of the found activation energies of the stabilizer decrease resulting from thermolytical ester decomposition. Comparison of the activation energies for each nitration site on AHP ring with QM calculated bond dissociation enthalpies.

Modelling with three second order reactions in parallel				
Ring position	**2**	**3**	**6**	**A_i weighted average**
Weighting by A_i	0.378	0.177	0.445	1
Ea [kJ mol^{-1}]	150	103	164	147.9
lg(Z [h^{-1}])	22.289	13.959	23.051	21.154
BDEnth [kJ/mol]	160.8	133.0	174.4	According to QM calculation [1]

In Fig. 7 the Arrhenius plots of the reaction rate constants of the three nitration reactions of the indicator, the aromatic dye are shown. Because of different activation energies the slopes are different and some intersection of the Arrhenius lines occur. One lies around 75°C. This can cause also a bend in Arrhenius plots with suitable measurement quantities. In Fig. 8 the decrease of the NE groups at the three specific positions on the AHP ring of NC can be seen. The order of stability of the three AHP ring sites is now twofold

> with regard to activation energy and bond dissociation enthalpy: C6 > C2 > C3
> with regard to degradation rates of the three sites: C6 > C3 > C2

The results presented here are described in more detail in the reference [4].

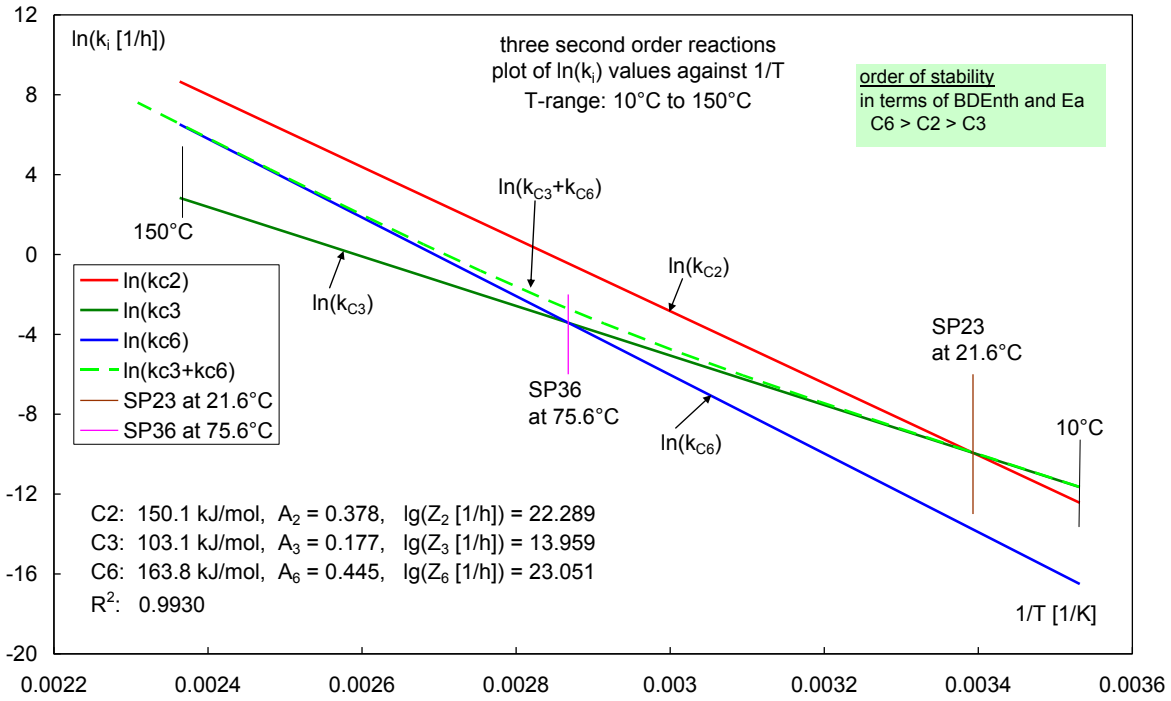

Figure 20-7: Arrhenius plots of the reaction rate constants of the three nitration reactions of the indicator molecule, the aromatic dye.

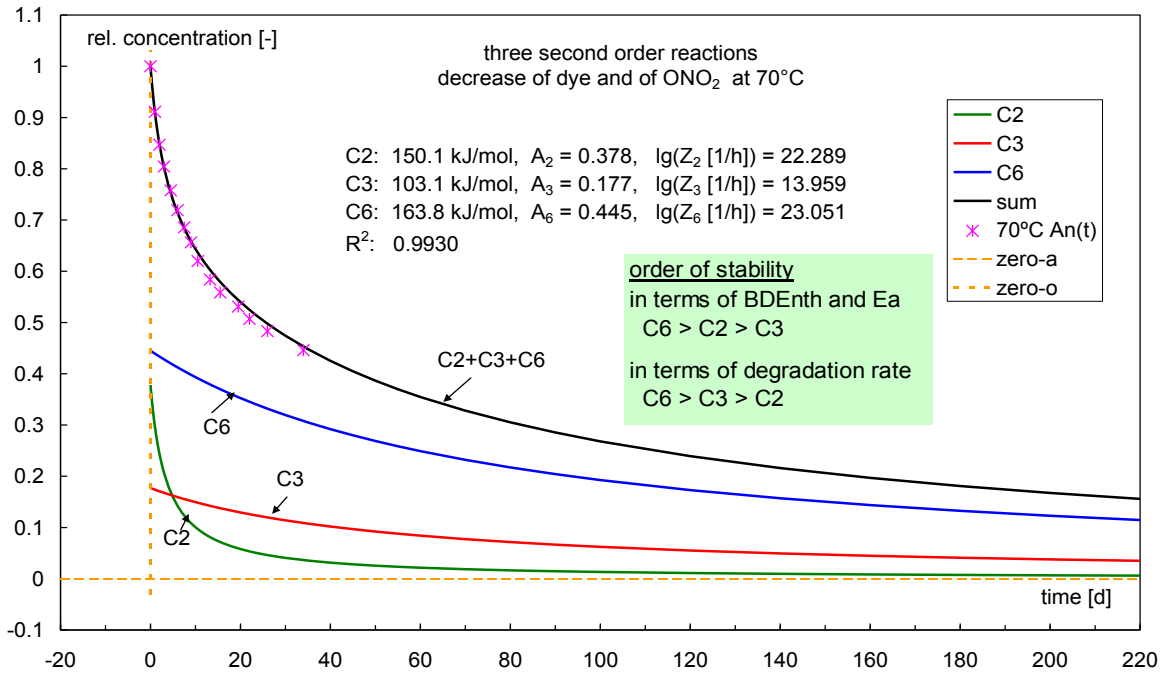

Figure 20-8: Decrease of the NE groups at the three specific positions on the AHP ring of NC. The order of stability of the three AHP ring sites is twofold:
> with regard to activation energy and bond dissociation enthalpy: C6 > C2 > C3
> with regard to degradation rates of the three sites: C6 > C3 > C2.

3.0 REACTION KINETIC DESCRIPTIONS FOR STABILIZER CONSUMPTION AND MEAN MOLAR MASS DECREASE

Stabilizer decrease is one of the best properties of a NC-based propellant to determine the residual safe in-service times. As long as enough stabilizer is present, the danger of self-ignition is minimized or even not present. There may be other properties controlling the in-service time, as surface treatment substances with gun propellants. But for db rocket propellants contained in the motor case one of the most important properties is stabilizer consumption and also chain scission of the NC. The reduction in NC chain length reduces the mechanical properties strain at break and stress at break in a correlated way with mean molar mass decrease. One problem may be the migration of plasticizer from the propellant into the liner and the isolation in case bonded configurations. This may reduce the bonding strength of the propellant to the liner and debonding may occur.

To make predictions of residual in-service times the procedure is as follows: One chooses the suitable measurement quantity, for example stabilizer decrease and molar mass degradation. One ages the material at some not to high temperatures, say 60°C, 70°C, 80°C and 90°C. Samples aged at different times are taken out and analysed with respect to stabilizer content (via extraction and HPLC analysis) and molar mass decrease, done via GPC (gel permeation chromatography). Then kinetic models are applied to describe the data and one obtains Arrhenius parameters, which allow the prediction of times to reach the wished or allowed conversions for stabilizer content and molar mass decrease.

In Table 3 the most used kinetically based models are compiled for stabilizer decrease and molar mass decrease, the last based on random chain splitting by chain element decomposition and a second model, which considers also chain recombination. Table 4 shows the integrated rate equations which can be used immediately.

Most of the equations in Table 3 and Table 4 need the use of non-linear fit algorithm. The best is to use all models with such a tool. The so-called linearization by logarithmic transformation should or better must be avoided. This procedure is still widely used with model ‘S: exponential’ and also model ‘S: nth order’. By this, the weighting of the data is strongly changed by fitting the regression lines. The model with number 5 in Table 3 or 4 is from all model for stabilizer decrease the most correct one. It considers the decomposition of the nitrate group and the reaction of the stabilizer. The other models do not consider the decomposition of the NE group. They are purely phenomenological to achieve the description of the course of the stabilizer, this holds also for the so-called AOP-48 model [5]. They are called here parametric models, see also [6, 7].

Figure 9 shows a comparison of three models of the type of description of a typical stabilizer decrease. Also 2-NO_2-DPA and Ak II show the same principle course of decrease, only the time scale differ. Qualitatively and quantitatively the model ‘S: exponential + linear’ describes these data best. The two models ‘S: nth order’ and ‘S extended’ show a tailing towards longer times, which seems not justified from the course of the data. To get an objective assessment of the description quality of a chosen model one must apply so-called information criteria, discussed in next section.

Table 20-3: Models to describe stabilizer consumption and molar mass decrease – kinetic rate expressions

Eq.	kinetic rate equation	kinetic type	name of model, type suitability, how to handle
1	$\frac{dS(t)}{dt} = -k_1 \cdot S(t) - k_0$	first + zero order, **two** reactions	**'S: exponential + linear', parametric** very suitable, easy to handle
2	$\frac{dS(t)}{dt} = -k_1 \cdot S(t)$	first order, **one** reaction	'S: exponential', parametric limited suitable, easy to handle
3	$\frac{dS(t)}{dt} = -k_0$	zero order, **one** reaction	**'S: linear', parametric** conditioned suitable, easy to handle
4	$\frac{dS(t)}{dt} = -k^{I} \cdot S(t)^{n}$	nth order, **one** reaction	**'S: nth order', parametric** good suitable, easy to handle
5	$\frac{dS(t)}{dt} = -k_{SP} \cdot S(t) \cdot (S(t) + NE(0) \cdot k_{NE} \cdot t)$	**two** reactions, model describes NE decomposition and consumption of S; this is the correct reaction kinetic base	**'S: extended', with reaction kinetic base** suitable, to handle with advanced fit codes (for example Origin™, Origin Lab Corp.)
6	$\frac{d\left(\frac{Mn(t,T)}{m}\right)}{dt} = -k_{Mn}(T) \cdot \left(\left(\frac{Mn(t,T)}{m}\right) + \left(\frac{Mn(t,T)}{m}\right)^2\right)$	chain splitting by random chain element decomposition	**'Mn: chain splitting', reaction kinetic base** suitable, easy to handle
7	$\frac{d\left(\frac{Mn(t)}{m}\right)}{dt} = -\left(k_{M1} + k_{M2} \cdot \exp(+k_{M1} \cdot t) \cdot \frac{m}{Mn(0)}\right) \cdot \left(\frac{Mn(t)}{m}\right)^2 - (k_{M1} - k_{M2}) \cdot \left(\frac{Mn(t)}{m}\right)$	chain splitting (CS) by random chain element decomposition (ED) and chain recombination (CR)	**'Mn: CS by ED and CR', reaction kinetic base** suitable, easy to handle

Table 20-4: Models to describe stabilizer consumption and molar mass decrease – integrated expressions. Model no 6 describes the decrease of mean molar mass Mn (number average) of a polymer by random chain scission by chain element (monomer) decomposition. Model no 7 has the same base as model no 6, but in addition chain recombination can occur.

Eq.	equation	time t_0 to $y_S = S(t)/S(0) = 0$	$ty_S(T)$ to reach, $y_S = S(t,T) / S(0)$
1	$S(t,T)=\left(S(0)+\frac{k_0(T)}{k_1(T)}\right)\cdot\exp\left(-k_1(T)\cdot t\right)-\frac{k_0(T)}{k_1(T)}$	$t_0(T)=\frac{1}{k_1(T)}\cdot\ln\left(\frac{S(0)\cdot k_1(T)}{k_0(T)}+1\right)$	$ty_S(T)=\frac{1}{k_1(T)}\cdot\ln\left(\frac{1+\frac{k_0(T)}{S(0)\cdot k_1(T)}}{y_S+\frac{k_0(T)}{S(0)\cdot k_1(T)}}\right)$
2	$S(t,T)=S(0)\cdot\exp\left(-k_1(T)\cdot t\right)$	$t_0(T)\rightarrow\infty$	$ty_S(T)=\frac{1}{k_1(T)}\cdot\ln\left(\frac{1}{y_S}\right)$
3	$S(t,T)=S(0)-k_0(T)\cdot t$	$t_0(T)=\frac{S(0)}{k_0(T)}$	$ty_S(T)=\frac{S(0)}{k_0(T)}\cdot(1-y_S)$
4	$S(t,T)=S(0)\cdot\left[1-(1-n)\cdot k(T)\cdot t\right]^{\left(\frac{1}{1-n}\right)}$ with $k(T)=\frac{k'(T)}{S(0)^{1-n}}$	$t_0(T)=\frac{1}{k(T)}\left(\frac{1}{1-n}\right)$ only for $n<1$	$ty_S(T)=\frac{1}{k(T)}\cdot\frac{1-(y_S)^{1-n}}{1-n}$ only for $n<1$
5	$S(t)=\frac{\sqrt{\exp\left(-NE(0)\cdot k_{NE}\cdot k_{SP}\cdot t^2\right)}}{\frac{1}{S(0)}+\sqrt{\frac{\pi}{2}}\cdot\frac{k_{SP}}{NE(0)\cdot k_{NE}}}\cdot\operatorname{erf}\left(\sqrt{\frac{NE(0)\cdot k_{NE}\cdot k_{SP}}{2}}\cdot t\right)$	$t_0(T)\rightarrow\infty$	no closed form for $ty_S(T)$
6	$Mn(t,T)=\frac{m}{\left(1+\frac{m}{Mn(0)}\right)\cdot\exp\left(+k_{Mn}(T)\cdot t\right)-1}$	$t_0(T)\rightarrow\infty$	$ty_{Mn}(T)=\frac{1}{k_{Mn}(T)}\cdot\ln\left(\frac{\frac{1}{y_{Mn}}+\frac{Mn(0)}{m}}{1+\frac{Mn(0)}{m}}\right)$
7	$\frac{Mn(t)}{m}=\frac{\exp\left(-k_{M1}\cdot t\right)}{\frac{m}{Mn(0)}+\frac{k_{M1}}{k_{M1}-k_{M2}}\cdot\left(\exp\left(-k_{M2}\cdot t\right)-\exp\left(-k_{M1}\cdot t\right)\right)}$	$t_0(T)\rightarrow\infty$	no closed form for $ty_{Mn}(T)$

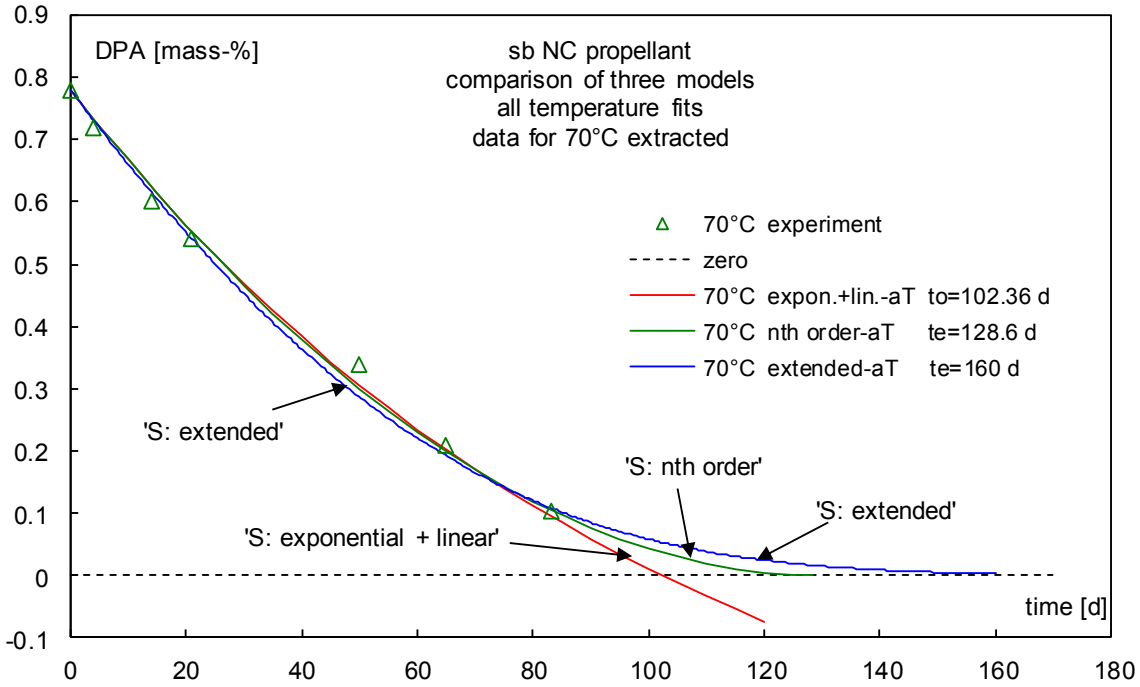

Figure 20-9: Comparison of three description models for stabilizer decrease: 'S: exponential+linear', 'S: nth order' (AOP-48 model), 'S: extended'. Depending on the quality of ageing, extraction and HPLC determination, the difference between the models reveal most evidently at low concentrations. But also the description quality of the course is different. This difference is quantifiable only with methods based on information criteria.

3.1 Information criteria to determine the best model out of a set of models

To describe any measurement data by models or parametric equations is mostly a necessity for the interpretation and further evaluations of the data. There is often the case that several models may be applicable and the question arises, which model is the better one. Besides many criteria to argue for one or another model there are objective methods for the assessment of the description quality for models in comparison. Such methods are based on information theoretical conclusions and two criteria have proven helpful. One has been developed by Hirot(s)ugu Akaike and it is called Akaike Information Criterion (AIC). The other method is based on the early work of Thomas Bayes, which was adapted by Gideon Schwarz to the framework of an information criterion and is named Bayes Information Criterion (BIC).

The two information criteria serve for model selection among a finite set of models. The selection method for both is based on the likelihood function. When fitting models, it is possible to increase the likelihood (here means description quality) by adding parameters. But doing so may result in overfitting. Both BIC and AIC resolve this problem by introducing a penalty term for the number of parameters in the model; the penalty term is larger in BIC than in AIC. Important to note is that the IC are applied relatively for a set of models. This means one has to compare always at least two models. The assessment uses a so-called statistical weight wA_i, wAc_i or wB_i for each model i. The higher the weight for a model the better is the description by this model. See [8] for further reading

3.1.1 Akaike information criterion (AIC)

The basic AIC is given in Eq.(3). The first term comes from the likelihood function; the second term is the penalty term. FQS means 'Fehlerquadratsumme', in English SSD, sum of squared deviations. Quantity n is the the number of data points, p is the number of fit parameters.

$$AIC = n \cdot \ln\left(\frac{FQS}{n}\right) + 2 \cdot (p+1) \tag{3}$$

A version with higher penalty term is shown in Eq.(4). It should be used when the number of data n is low and n/p << 1000.

$$AICc = n \cdot \ln\left(\frac{FQS}{n}\right) + 2 \cdot (p+1) + \frac{2 \cdot p \cdot (p+1)}{n-p-1} \tag{4}$$

The normalized statistical AIC weight is named wA_i or wAc_i of a model *i* among a set of *u* models chosen for the quality test is obtained by Eq.(5). It uses the 'distance' ΔA_i or ΔAc_i between the 'best' model with smallest AICc, called $AICc_{min}$, and the $AICc_i$ of model *i*, Eq.(6). The quantity $\exp(-\Delta A_i/2)$ or $\exp(-\Delta Ac_i/2)$ is the relative maximum likelihood of model *i* in comparison with the other models.

$$wAc_i = \frac{\exp(-\Delta Ac_i/2)}{\sum_{i=1}^{u} \exp(-\Delta Ac_i/2)} \tag{5}$$

$$\Delta Ac_i = AICc_i - AICc_{min} \tag{6}$$

3.1.2 Bayes (Schwarz-Bayes) information criterion (BIC)

The BIC is the same way constructed with likelihood term and penalty term, see Eq.(7). The last differs from AIC. Often the term $\ln(2\pi)$ is set to zero which increases the penalty. Statistical weight, Eq.(8) and determination of the 'distance' ΔB_i, Eq.(9), are analogously to AIC.

$$BIC = n \cdot \ln\left(\frac{FQS}{n}\right) + p \cdot (\ln(n) - \ln(2\pi)) \tag{7}$$

$$wB_i = \frac{\exp(-\Delta B_i/2)}{\sum_{i=1}^{u} \exp(-\Delta B_i/2)} \tag{8}$$

$$\Delta B_i = BIC_i - BIC_{min} \tag{9}$$

3.1.3 General remarks on the information criteria

The lower the AIC or AICc or BIC value the better is the assessment of the model. The more fit parameters are used the higher the AIC or AICc or BIC value. This means formulated in information content about the data: The higher the AIC or AICc or BIC of a model, the higher the information loss about the data. The difference between AIC and BIC is the different penalty term. Sometimes the part $\ln(2\pi)$ in BIC penalty term is omitted, which increases the penalty. AIC and BIC can tell nothing about the quality of the model in an absolute sense. If all candidate models fit poorly, AIC and BIC will not give any warning about this. Further, there is no selection of a possible 'true' model. The general assumption about the selected models to be tested is that none of them is the 'true' model. The only assessment result is in terms

of information loss in using a description (model) for the experimental data. This means that the entity of the experimental data itself has the highest degree of information. Any regression or data reduction or model description reduces this amount of information (information is in the context of thermodynamics an extensive quantity). AIC and BIC help to select the description or the model, which provides with the *least information loss* about the data. In reference [8] more details and worked out examples are given.

3.2 Kinetic description of 2-NO_2-DPA decrease in db rocket propellant

The use of the information criteria to describe the data on stabilizer decrease for a db RP are now presented. Figure 10 shows the data of 2-NO_2-DPA decrease and the descriptions with models 'S: exponential + linear' and 'S: exponential'. It is clearly to see that model 'S: exponential' provides with not good description of all the data, in spite of omitting the data marked with little arrows. Including these data, the description is worse with model 'S: exponential'. These data were not omitted with model 'S: exponential + linear'.

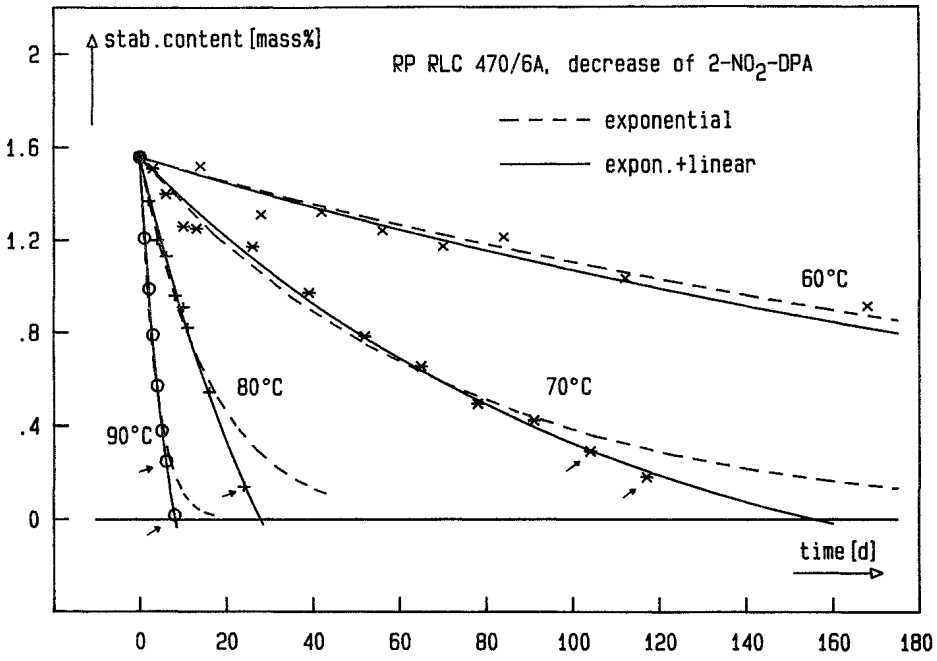

Figure 20-10: Decrease of stabilizer 2-NO2-DPA in a db RP and the description of the data with two models. Date marked with arrows have been omitted with model 'S: exponential' but not with the other model [9].

The quality of the descriptions of all five models compiled above in Table 3 and 4 for the 2-NO_2-DPA decrease in the db RP RLC 470 at 70°C, 80°C and 90°C is now assessed with AIC and BIC. The data description is done at once with all data at all temperatures. The fit parameters are the Arrhenius parameters of the rate constants and the reaction order, when it applies. From the five models the model 'S: exponential + linear' is assessed overwhelmingly as the best model in the set of five models. With the weights of > 99% in AIC, AICc and BIC, it surmounts all other models. Model 'S: nth order' is with its values of 0.005 to 0.009 far away.

Table20-5: Results of the model assessments used to describe the stabilizer decrease data of db rocket propellant RLC 470. 2-NO_2-DPA decrease at 70°C, 80°C and 90°C. Data fitted at once with all temperatures and the determination of the Arrhenius parameters of the reaction rate constants of the models, and the reaction order, when it applies.

Model → ↓ Quantity	linear k	expon. k	expn. + linear, k_1, k_0	nth order k, n_O	extended k_N, k_S	row summations
n	30	30	30	30	30	
p	2	2	4	3	4	
SD^2	0.01161	0.01197	0.00204	0.00294	0.0045	
R^2	0.94909	0.94748	0.99168	0.98758	0.98165	
Ea / Ea_1 /Ea_N [kJ/mol]	146.8 ± 3.6	129.3 ± 1.3	149.8 ± 7.7	144.6 ± 1.3	144.0 ± 7.1	
lg(Z_J [m.-%/d]	20.473 ± 0.41	17.918 ± 0.19	20.741 ± 0.78	20.093 ± 0.13	20.384 ± 0.71	
n_O [-]	-	-	-	0.5113 ± 0.25	-	
Ea_0 / Ea_S [kJ/mol]	-	-	150.5 ± 15.9	-	139.3 ± 6.2	
lg(Z_J [m.-%/d]	-	-	20.327 ± 1.50	-	19.121 ± 0.77	
FQS (SSD)	0.32508	0.33516	0.05304	0.07938	0.117	
AICc	-129.302	-128.386	-178.537	-169.118	-154.803	
exp(-ΔAci/2)	2.036E-11	1.288E-11	1	0.0090	7.019E-06	1.0090
wAci	2.018E-11	1.276E-11	0.991	0.009	6.956E-06	1
AIC	-129.746	-128.830	-180.137	-170.041	-156.403	
exp(-ΔAi/2)	1.142E-11	7.225E-12	1	0.0064	7.019E-06	1.0064
wAi	1.135E-11	7.179E-12	0.994	0.006	6.974E-06	1
BIC	-132.620	-131.704	-183.884	-173.351	-160.150	
exp(-ΔBi/2)	7.381E-12	4.669E-12	1	0.0052	7.019E-06	1.0052
wBi	7.343E-12	4.645E-12	0.995	0.005	6.983E-06	1

k and ki: reaction rate constants of the model

no reaction order of the model 'S: nth order'

n number of data used

p number of fit parameters of the model (the freely varied ones)

SD^2 squared standard deviation or variance, $SD^2 = FQS/(n-p)$

R^2 coefficient of determination;

$$R^2 = 1 - FQS \Big/ \sum_i^n \{y(x_i) - M(y(x_i))\}^2 \; ; \quad M(y(x_i)) = \sum_i^n y(x_i) \Big/ n$$

FQS Fehlerquadratsumme, equal to SSD (sum of squared deviations)

$$FQS = \sum_i^n (y(x_i) - f_{cal}(x_i))^2$$

3.3 Kinetic description of a sigmoid-type stabilizer decrease

Recently the sigmoid stabilizer decrease was stated to occur. This is still not proven. Anyway, if such a behaviour is real with stabilizers then a correct modelling can describe such a behaviour on a reaction kinetic sound base [10]. In order to describe the consumption of the primary stabilizer (which means added stabilizer at production), an extended modelling is appropriate considering the two governing reactions: (1) decomposition of NC and (2) the bimolecular reaction of the stabilizer with the dangerous product P. A good stabilizer is of such quality that the concentration level of P is so low that the autocatalytic reaction does not occur and Eq.(10) is valid. It shows only intrinsic NC decomposition and the action of the stabilizer S.

$$\left.\begin{aligned} NC &\xrightarrow{k_{NC}} P + NC - R \\ S + P &\xrightarrow{k_{Su}} S\text{-}P \end{aligned}\right\} \qquad (10)$$

This is the basic kinetic approach and it is not further to simplify. One needs at least two reaction rate constants, which means two reactions, to have the kinetically correct formulation of NC decomposition and stabilizer action. The system of differential equations of Eq.(10) is shown in Eq.(11). The Eq.(12) shows the sequence of rearrangements, which lead to the final differential equation Eq.(13).

$$\left.\begin{aligned} \frac{dNC(t)}{dt} &= -k_{NC} \cdot NC(t) \\ \frac{dP(t)}{dt} &= +k_{NC} \cdot NC(t) - k_{Su} \cdot S(t) \cdot P(t) \\ \frac{dS(t)}{dt} &= -k_{Su} \cdot S(t) \cdot P(t) \end{aligned}\right\} \qquad (11)$$

$$\left.\begin{aligned} &NC(t) = NC(0) \cdot \exp(-k_{NC1} \cdot t) \\ &\frac{dP(t)}{dt} - \frac{dS(t)}{dt} = k_{NC} \cdot NC(t) \\ &\text{The solution is :} \\ &P(t) - S(t) = C - NC(0) \cdot e^{-k_{NC} \cdot t} \\ &\text{with C as integration constant :} \quad C = NC(0) + P(0) - S(0) = NC(0) + D \\ &\text{For the decrease of S we get :} \\ &\frac{dS(t)}{dt} = -k_{Su} \cdot S(t) \cdot \left(S(t) + C - NC(0) \cdot e^{-k_{NC} \cdot t} \right) \end{aligned}\right\} \qquad (12)$$

$$\frac{dS(t)}{dt} = -k_{Su} \cdot S(t) \cdot (S(t) + D) - k_{Su} \cdot S(t) \cdot NC(0) \cdot \left(1 - e^{-k_{NC} \cdot t}\right) \qquad (13)$$

Eq.(13) could be already used to determine the two reaction rate constants, but it is very useful to normalize the stabilizer concentration by its initial value S(0). This is shown in Eq.(14). Further, some expressions are introduced as well as the normalized rate constant k_S, Eq.(15); which has the dimension 1/time and no longer incorporates the reciprocal concentration. Finally Eq.(16) is obtained, which can be easily

rearranged to Eq.(17), which shows the obvious Bernoulli character of this Deq.

$$\frac{d\left(\frac{S(t)}{S(0)}\right)}{dt} = -k_{Su}\cdot S(0)\cdot\frac{S(t)}{S(0)}\cdot\left(\frac{S(t)}{S(0)}+\frac{D}{S(0)}\right)-k_{Su}\cdot S(0)\cdot\frac{S(t)}{S(0)}\cdot\frac{NC(0)}{S(0)}\cdot\left(1-e^{-k_{NC}\cdot t}\right) \qquad (14)$$

$$k_S = k_{Su}\cdot S(0),\quad Sr(t)=\frac{S(t)}{S(0)},\quad CS=\frac{NC(0)}{S(0)}\quad Dn=\frac{P(0)-S(0)}{S(0)}=\frac{P(0)}{S(0)}-1 \qquad (15)$$

$$\frac{dSr(t)}{dt} = -k_S\cdot Sr(t)\cdot\left(Sr(t)+Dn\right)-k_S\cdot Sr(t)\cdot CS\cdot\left(1-e^{-k_{NC}\cdot t}\right) \qquad (16)$$

$$\frac{dSr(t)}{dt} = -k_S\cdot Sr(t)^2-k_S\cdot\left(Dn+CS\cdot\left(1-e^{-k_{NC}\cdot t}\right)\right)\cdot Sr(t) \qquad (17)$$

The integration of the Bernoulli-type Eq.(17) with Sr(0) = 1 or here with Sr(0) = Sro, which is set mostly and reasonably to 1, gives Eq.(18), which is named **model 'S: bimolecular, NC first order'**. Note: the development of Eq.(16 and Eq.(18) allows to have an initial concentration of P greater than zero.

$$Sr(t)=\frac{\exp\left(\frac{k_S\cdot CS}{k_{NC}}\right)\cdot\exp\left(-k_S\cdot\left(\frac{CS\cdot\exp(-k_{NC}\cdot t)}{k_{NC}}\right)-k_S\cdot(CS+Dn)\cdot t\right)}{\frac{1}{Sro}+\exp\left(\frac{k_S\cdot CS}{k_{NC}}\right)\cdot\int_0^t\exp\left(-k_S\cdot\left(\frac{CS\cdot\exp(-k_{NC}\cdot t')}{k_{NC}}\right)-k_S\cdot(CS+Dn)\cdot t'\right)\cdot k_S\cdot dt'} \qquad (18)$$

Because NC decomposes slowly, especially with a good stabilizer, the following approximation is possible without loss in quality of the description, Eq.(19), which results in the Eq.(20) and rearranged in the Eq.(21).

$$\left(1-e^{-k_{NC}\cdot t}\right)=\approx k_{NC}\cdot t \qquad (19)$$

$$\frac{dSr(t)}{dt} = -k_S\cdot Sr(t)\cdot\left(Sr(t)+Dn\right)-k_S\cdot Sr(t)\cdot CS\cdot k_{NC}\cdot t \qquad (20)$$

$$\frac{dSr(t)}{dt} = -k_S\cdot Sr(t)^2-k_S\cdot\left(Dn+CS\cdot k_{NC}\cdot t\right)\cdot Sr(t) \qquad (21)$$

The integration of the Bernoulli-type Eq.(21) with Sr(0) = 1 or here with Sr(0) = Sro, gives Eq.(22), which is named **model 'S: bimolecular, NC zero order'**.
Note: the quantity Dn may not be placed as Dn^2 under the square roots in the two error functions (erf). This holds for any quantity, which could appear with negative numbers.

$$Sr(t)=\frac{\exp\left(-k_S\cdot Dn\cdot t\right)\cdot\exp\left(-\frac{k_S\cdot k_{NC}\cdot CS\cdot t^2}{2}\right)}{\frac{1}{Sro}-\exp\left(\frac{k_S\cdot Dn^2}{2k_{NC}CS}\right)\sqrt{\frac{k_S\cdot\pi}{2k_{NC}CS}}\left[\operatorname{erf}\left(\sqrt{\frac{k_S}{2k_{NC}CS}}Dn\right)-\operatorname{erf}\left(\sqrt{\frac{k_S}{2k_{NC}CS}}Dn+\sqrt{\frac{k_Sk_{NC}CS}{2}}\cdot t\right)\right]} \qquad (22)$$

In Table 6 three data sets are given, with which the curves in Fig. 11 were established. They show the variability of Eq.(22). It can describe different sigmoid-type shapes and also immediately decreasing data, as

shown with data set 2. See Appendix A1 in [10] for determination of the parameters CS, S(0), Dn. For the NC(0) in CS the concentration of the nitrate ester groups at time zero is taken, means $ONO_2(0)$.

Table 20-6: Data sets used to illustrate the variety of courses of the model 'S: bimolecular, NC zero order'.

quantity	unit	data set 1	data set 2	data set 3
k_{NC}	1/d	0.002	0.008	0.008
k_S	1/d	0.1	0.01	0.01
NC(0) content in GP	mass-%	97.0	97.0	97.0
N content of NC	mass-%	13.1	13.1	13.1
$ONO_2(0)$ content in GP	mass-%	56.25	56.25	56.25
S(0)	mass-%/100%	0.02	0.02	0.02
P(0)	mass-%/100%	0.001	0.10	0.0
Sro = Sr(0)	-	1.0	1.0	1.0
CS = $ONO_2(0)$/S(0)	mass-%/mass-%	28.125	28.125	28.125
Dn = P(0)/S(0) - 1	-	-0.95	4.0	-1.0

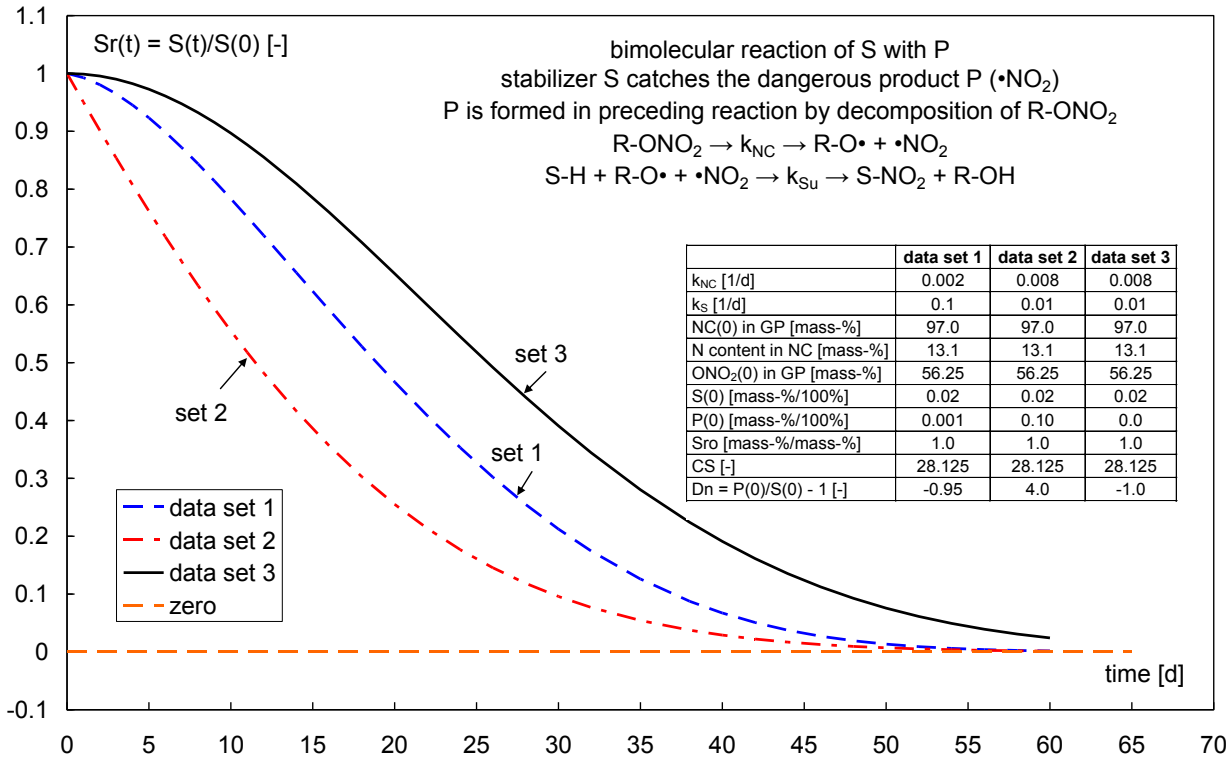

	data set 1	data set 2	data set 3
k_{NC} [1/d]	0.002	0.008	0.008
k_S [1/d]	0.1	0.01	0.01
NC(0) in GP [mass-%]	97.0	97.0	97.0
N content in NC [mass-%]	13.1	13.1	13.1
$ONO_2(0)$ in GP [mass-%]	56.25	56.25	56.25
S(0) [mass-%/100%]	0.02	0.02	0.02
P(0) [mass-%/100%]	0.001	0.10	0.0
Sro [mass-%/mass-%]	1.0	1.0	1.0
CS [-]	28.125	28.125	28.125
Dn = P(0)/S(0) - 1 [-]	-0.95	4.0	-1.0

Figure 20-11: Examples of curve shapes obtainable by model 'S: bimolecular, NC zero order'. The model is able to describe sigmoid-type decreasing data and pure monotonic decreasing data. The sigmoid-type shape is caused by retardation of the reaction of S with P during the start-up behaviour, because of producing P from NC first [10-1, 10-2].

4.0 SINGLE TEMPERATURE METHOD OF AOP-48 TO DETERMINE CHEMICAL STABILITY

In AOP-48, Edition 2 [5] a simplified method to assess relatively fast and easy the chemical stability of NC-based material is formulated. If the two criteria are fulfilled, the assessment is chemically stable for the next 10 years at isothermal storage (or kinetically equivalent temperature) at 25°C The test ageing is done by selecting a pair of test temperature and test time, given in a list in AOP-48. After ageing of the test sample, the following criteria apply.

Assessment criteria:

Residual content of stabiliser after the test ageing ≥ 0.2 mass-%
Relative stabiliser decrease during the test ageing ≤ 80 %

Both criteria must be fulfilled to achieve 'stable for the next 10 years at 25°C'.

Table 20-7: Example of the application of the simplified assessment method according to AOP-48, Ed. 2. For the two DBxxxx, the test ageing was performed at 85°C over 6 days. Data of DBxxxx from [12]. The DBE xxx were aged at 80°C over 10.6 days, data determined at ICT. All four tested materials fulfil the AOP-48 criteria.

Sample	stabilizer	Initial stabilizer content (before any ageing) [mass-%]	Stabilizer content after test ageing [mass-%]	Found relative stabilizer decrease [%]	Formal stabilizer content after 80% relative decrease [mass-%]	Assessment
Ageing at 85°C over 6 days						
DB2016	2-NO_2-DPA	1.75	0.711	59.4	0.35	stable over 10a at 25°C
DB2008	2-NO_2-DPA	1.9	1.465	22.9	0.38	stable over 10a at 25°C
Ageing at 80°C over 10.6 days						
DBE 470	Akardite II	1.91	1.47	23.0	0.38	stable over 10a at 25°C
DBE 40	2-NO_2-DPA	1.99	1.12	43.7	0.40	stable over 10a at 25°C
Criteria	Valid for all AOP-48 listed stabilizers	-	≥ 0.20	≤ 80	-	stable over 10a at 25°C

5.0 CORRELATION BETWEEN STABILIZER DECREASE, MOLAR MASS DECREASE AND CHANGE IN TENSILE PROPERTIES AT BREAK

In the following experimental data of a double base propellant DBE 44 from Bayern Chemie GmbH are shown, which confirm the connection between the properties stabilizer decrease, molar mass decrease of NC and mechanical tensile properties, which are determined by the polymeric character of NC. All the properties were determined from samples aged at the same time. The data have been published in [2].

Figure 12 shows the decrease of stabilizer AK II in DBE 44. This decrease is congruent with the decrease in mean molar mass of the NC in this propellant, which can be seen in Figure 13. As expected the mechanical properties strain at break and stress at break decrease analogously to the mean molar mass Mw, see Figure 14 and Figure 15, respectively.

To model the data, any deceasing function could be tried and checked via AIC and BIC if the model is adequate. Often the Layton formalism is tried. The Layton expression starts from a reference time-data value set t_0 and P_0 and correlates the following data at time t with value P according to Eq.(23).

$$P(t,T) = P_0(t_0,T) + L_P(T) \cdot \ln\left(\frac{t}{t_0}\right) \tag{23}$$

Note: the Layton constant L_P **is not a rate** constant. Is has the unit of the property P and not 1/time as with real rate constants.

Establishing the time ty(T) to reach the value P(ty(T)), means to make predictions

$$P(ty(T)) - P_0(t_0,T) = +L_P(T) \cdot \ln\left(\frac{ty(T)}{t_0}\right) \tag{24}$$

$$\frac{P(ty(T)) - P_0(t_0,T)}{L_P(T)} = \ln\left(\frac{ty(T)}{t_0}\right) \tag{25}$$

$$\frac{ty(T)}{t_0} = \exp\left(\frac{P(ty(T)) - P_0(t_0,T)}{L_P(T)}\right) \tag{26}$$

Introduction and definition of degree of property change y_P

$$y_P = \frac{P(ty(T))}{P_0(t_0,T)} \tag{27}$$

y_P ranges from 1 to 0 with decreasing P
y_P ranges from 1 upwards with increasing P

$$\frac{ty(T)}{t_0} = \exp\left(\frac{P_0(t_0,T) \cdot (y_P - 1)}{L_P(T)}\right) \tag{28}$$

Formal temperature parameterization of Layton constant L_P

According to Arrhenius

$$L_P(T) = Z_{L_P} \cdot \exp\left(-\frac{Ea_{L_P}}{R \cdot T}\right) \tag{29}$$

According to van't Hoff

$$L_P(T) = H_{L_P} \cdot F_{\Delta T}^{(T/\Delta T_F)} \tag{30}$$

For use of van't Hoff temperature parameterization, see [11]. The van't Hoff method is working, when the property change follows a two-mechanistic change in temperature. The range of temperature should not too large; a typical range is 15°C to 90°C or 100°C with NC-based materials. With HTPB-based binders,

the range is 20°C to 140°C, see [11] for more details.

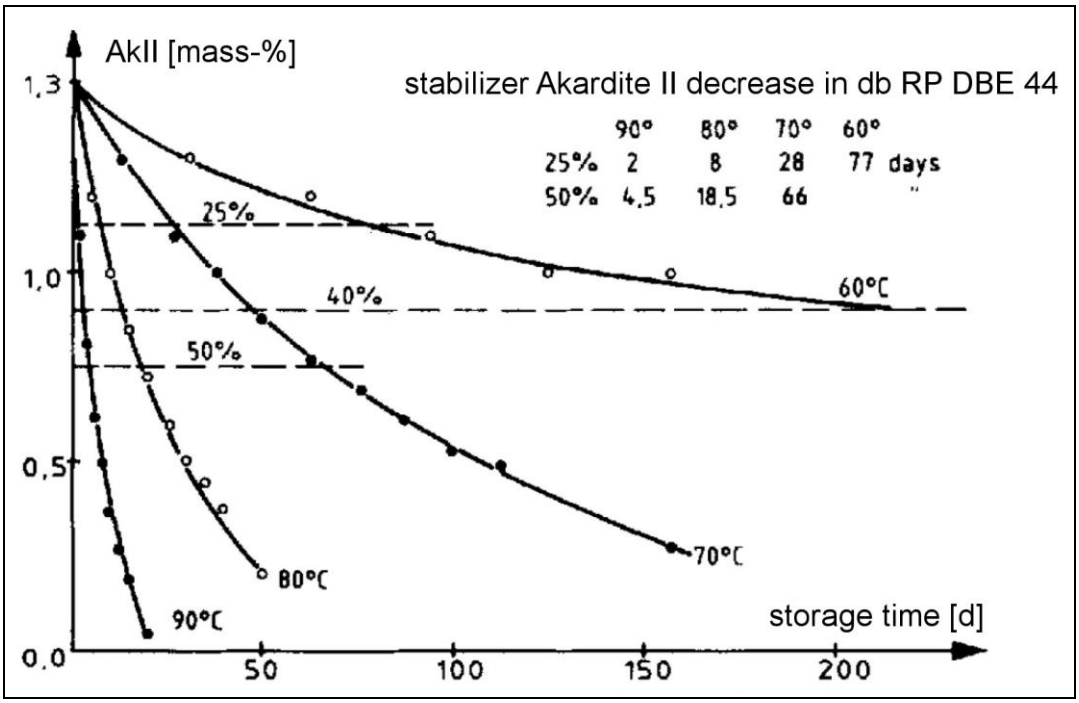

Figure 20-12: Decrease of stabilizer Ak II in db RP DBE 44 with ageing.

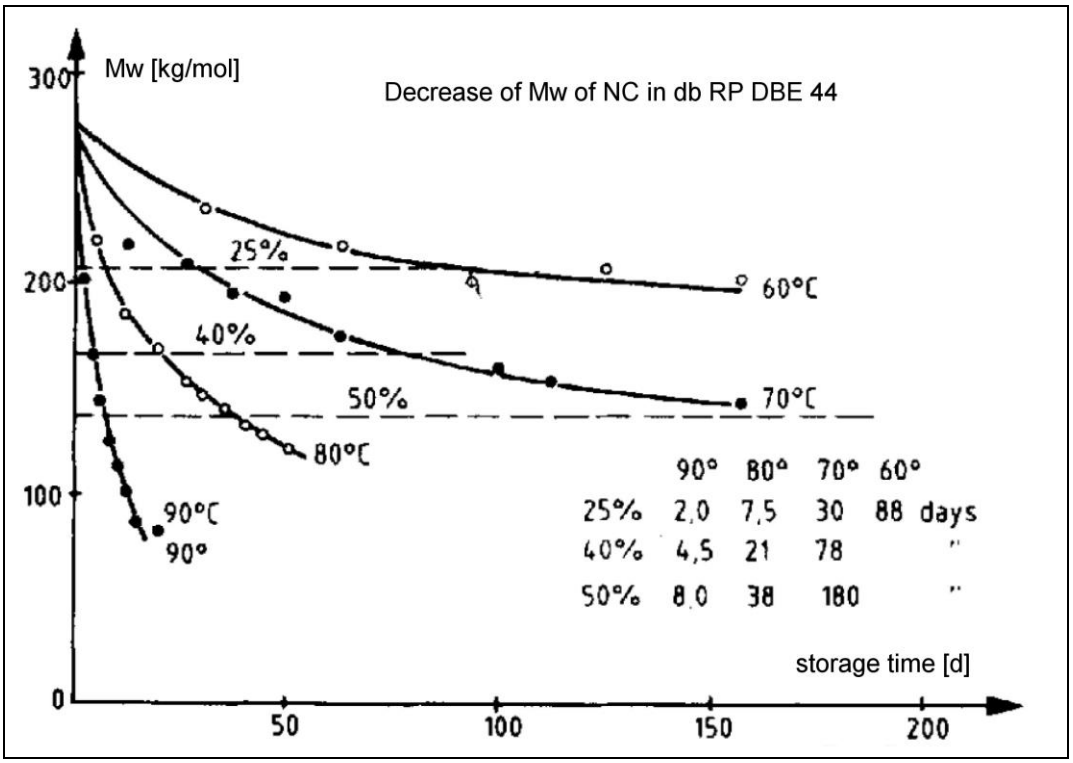

Figure 20-13: Decrease of mean molar mass Mw of NC in db RP DBE 44 with ageing.

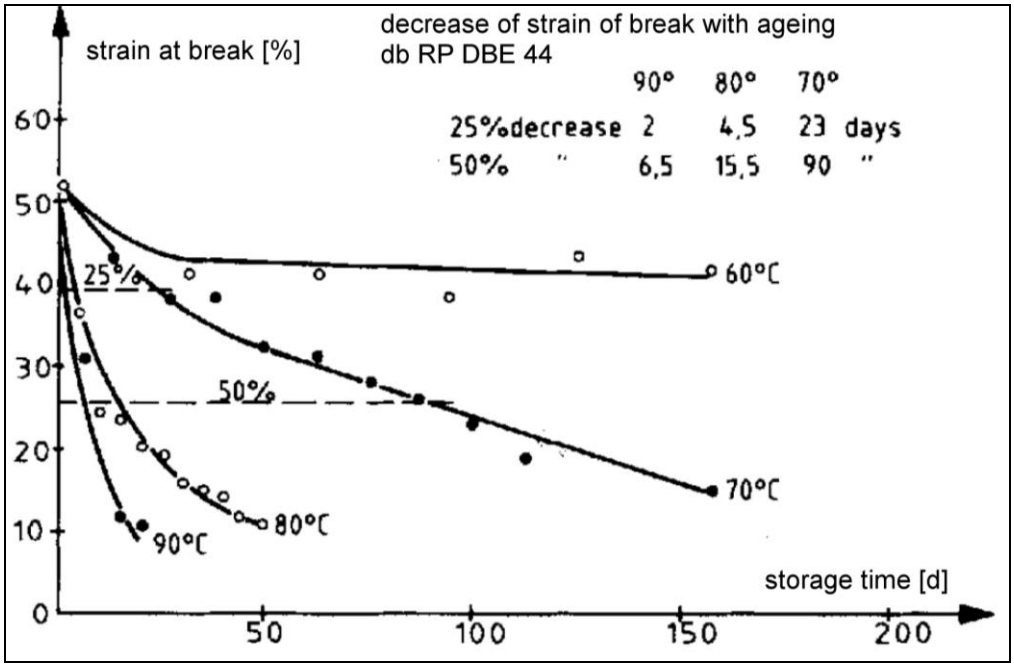

Figure 20-14: Decrease of strain at break with ageing of db RP DBE 44.

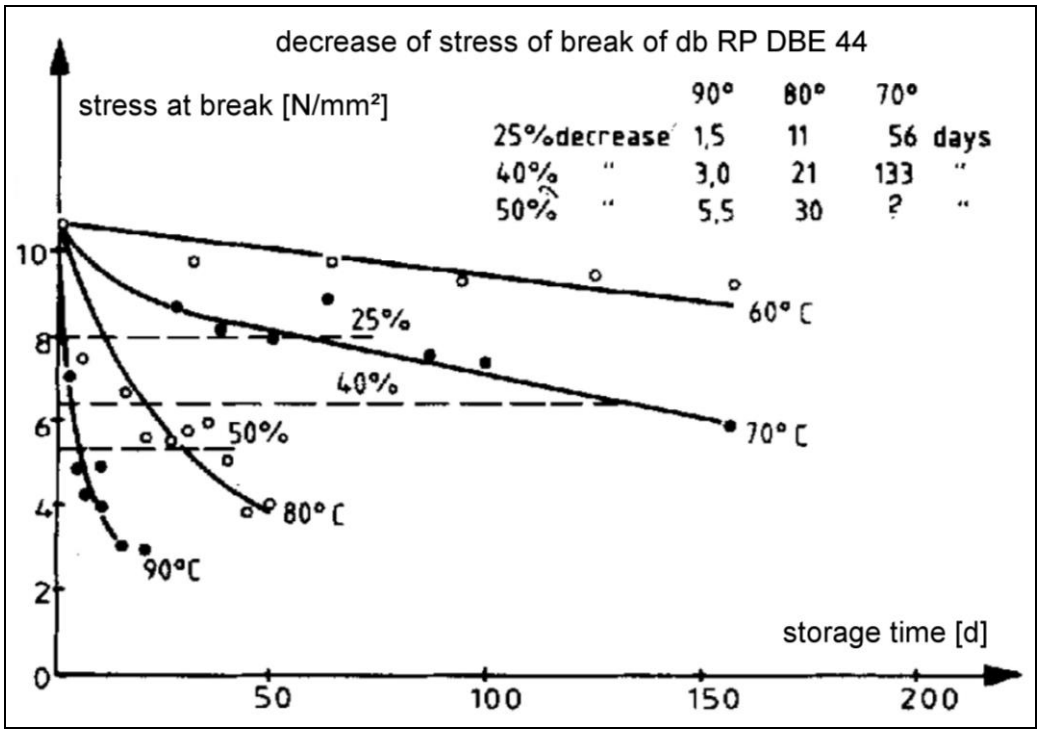

Figure 20-15: Decrease of stress at break with ageing of db RP DBE 44.

6.0 MASS LOSS AS AN INDICATOR FOR THE VERY END OF SAFE IN-SERVICE TIME AND AS STABILITY CRITERION AS WELL AS PREDICTION TOOL

In contrast to stabilizer decrease and molar mass degradation is mass loss as well at heat generation rate

and heat generation a so-called 'global' quantity, all decomposition effects are in summarized way 'collected' in the mass loss data. The same holds also for gas generation. Nevertheless is mass loss determined at low to medium temperatures a valuable quantity. The disadvantage is the data collection, normally done by remote weighing of vials with an analytical balance.

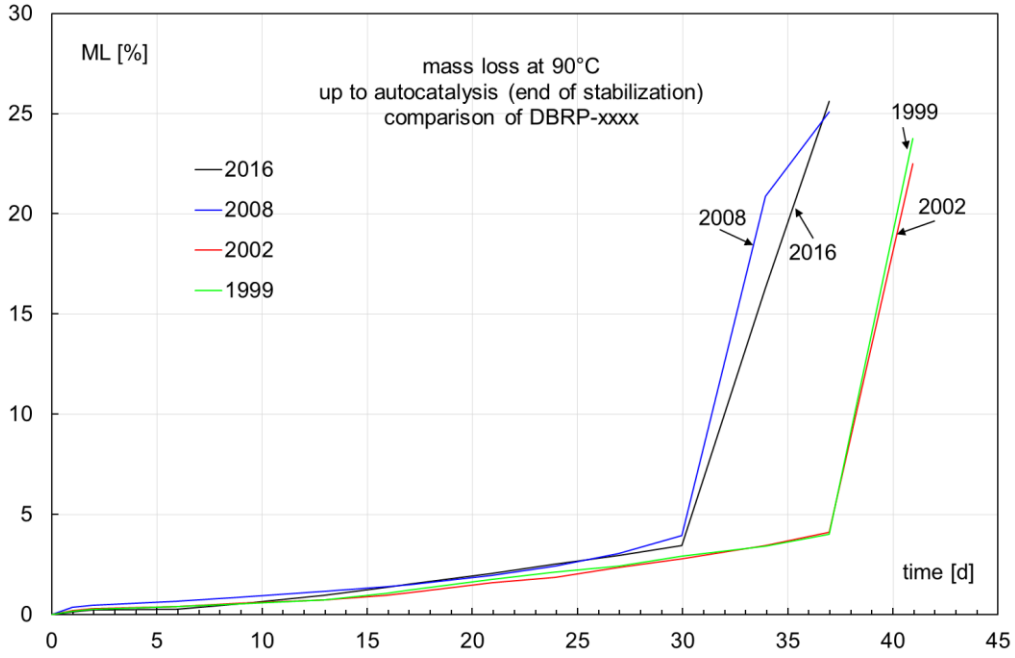

Figure 20-16: Mass loss at 90°C over 40 days of four db RP, stabilized with 2-NO2-DPA. After slow increase of ML during the time of active stabilizer action, the unstabilized phase follows with strong mass loss increase, the autocatalytic decomposition.

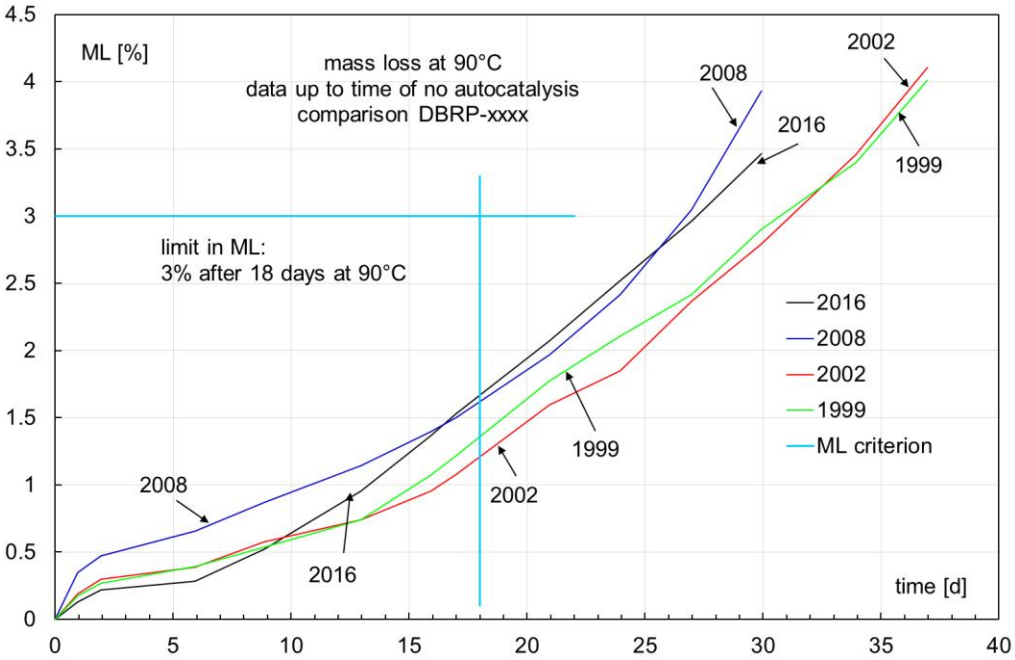

Figure 20-17: Mass loss at 90°C up to the time just before autocatalysis. All four propellant samples fulfil very well the demanding German stability criterion: over 18 days the ML must be below 3%. According to AOP-48 criteria this corresponds to about 50 years at 25°C.

Figure 16 shows a typical example of mass loss up to the time with accelerated mass loss increase, which is often called the state of autocatalysis. At the turn over from slow increase to fast increase all effective stabilizer is consumed, the material is from this point on unstabilized. On the other hand. up to this point the material is still useable. In the example of Figure 16 the four Brazilian db RP, stabilized with 2-NO_2-DPA, can be used up to 25 days at 90°C. This corresponds to 65 to 70 years at 25 °C. The four db RP are Brazilian ones and are the same as presented in [12] together with other evaluation. In part they have been investigated also, below further results are presented. In Figure 17 the four db RP are shown up to the time just before autocatalysis. The curves show a slight increasing rate.

The Figure 18 compares the mass loss (ML) of db RP manufactured all from the same company. The DBE 40 and RLC 470 have 2-NO_2-DPA as stabilizer, the two DBE 470 have Ak II as stabilizer. The first group has clearly lower mass loss evolution then the second group. In Figure 19 all the investigated db RP are compared. Again the group with 2-NO_2-DPA separates from the AkII stabilized samples. Another difference reveals Figure 20. AKII stabilized RP show much longer times until autocatalysis is reached. In this respect, Ak II is a better stabilizer than 2-NO_2-DPA. This effect is also found with stabilizer decrease, Ak II lasts longer than other stabilizers. But there are further important criteria to state the suitability of a stabilizer, see section 8.0. An interesting feature is shown by the ML curve of DBE 40, see Figures 18 and 19. At the beginning, up to14 days, the ML increases very slowly then around 15 days it turns to a second step with increased rate, but this is still in the range of the rates of the other RP formulations. It is not yet the change to autocatalysis, the state of completely unstabilized material. To explain this behaviour one can assume that the primary stabilizer is consumed after 14 to 15 days and then only the consecutive products, means higher nitrated ones, are active as stabilizers. This behaviour can be found also with the set of the four DBRPxxxx propellants, but not so pronounced as with DBE 40.

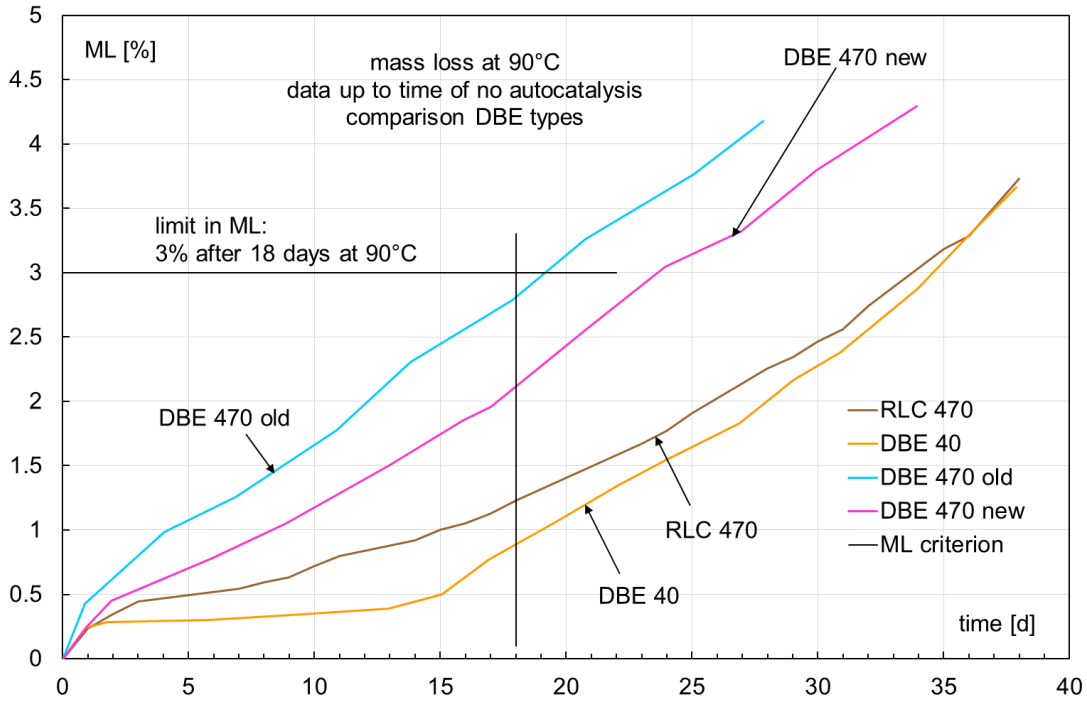

Figure 20-18: Mass loss at 90°C up to the time just before autocatalysis of four German db RP propellants manufactured by Bayern-Chemie GmbH, Aschau am Inn. All fulfil the German ML criterion. One can identify two groups: DBE 470 new and old are stabilized with Ak II, the DBE 40 and RLC 470 are stabilized by 2-NO2-DPA. The last group shows at begin lower mass loss than the first group.

The AK II stabilized (DBE 470) samples show a long time period with more or less steady increase of ML without an accelerating component, see Figure 20. This is also a characteristic feature of stabilizer AK II.

These linear parts of ML can be used also in prediction work, when ML is determined at several temperatures. The procedure is shown in detail in [13] together with [14] because the application of time-temperature profiles. The formalism is used also in [15] for the determination of Arrhenius parameters.

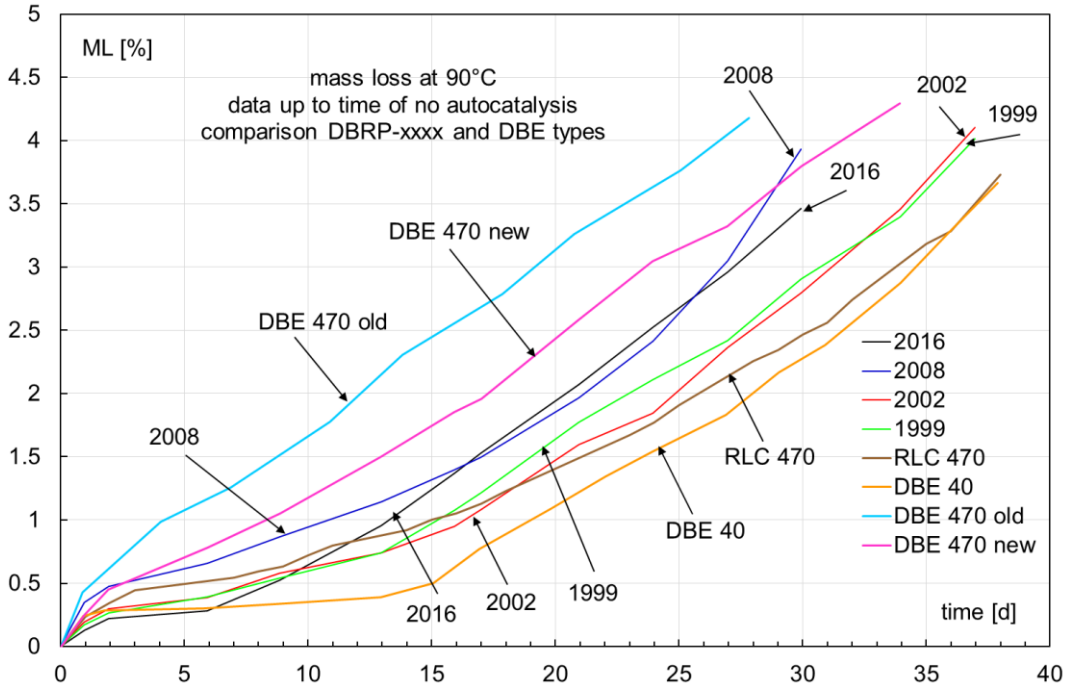

Figure 20-19: Comparison of db RP with ML at 90°C. The samples stabilized with 2-NO2-DPA are always below the ones stabilized with AkII.

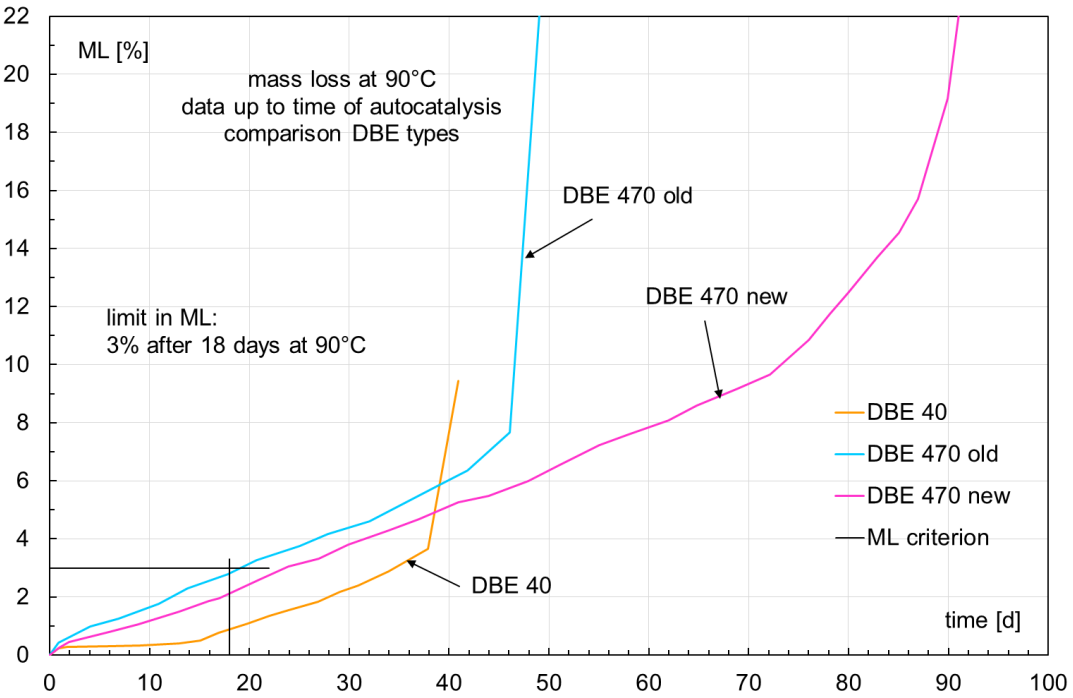

Figure 20-20: Mass loss of db RP of DBE type. DBE 40 is 2-NO2-DPA stabilized the DBE 470 are AkII stabilized. The last group comes much later to the point of autocatalysis the 2-NO2-DPA stabilized propellants. But the lower mass loss indicates lower gas generation, which is a very advantageous property for db RP.

7.0 HEAT GENERATION RATE AS INDICATOR FOR CHEMICAL STABILITY OF DB RP

Heat generation rate is as mass loss and gas generation a so-called 'global' property in comparison to the specific property stabilizer decrease. A summarized effect is measured which includes many endothermal and exothermal reactions. The different stabilizers produce different 'patterns' which indicate a high influence of the stabilizer reactions itself. Therefore, the situation may arise where HGR alone is not enough to characterize the stability of material. Other methods should always complement HGR evaluations. Worked out procedures as NATO STANAG 4582 (Heat Flow Microcalorimetry STANAG) [16] are valid only for NC-based material. More about the 'construction' of the STANAG 4582 can be found in [17]. Also prediction with time-temperature profiles can be made, see [18].

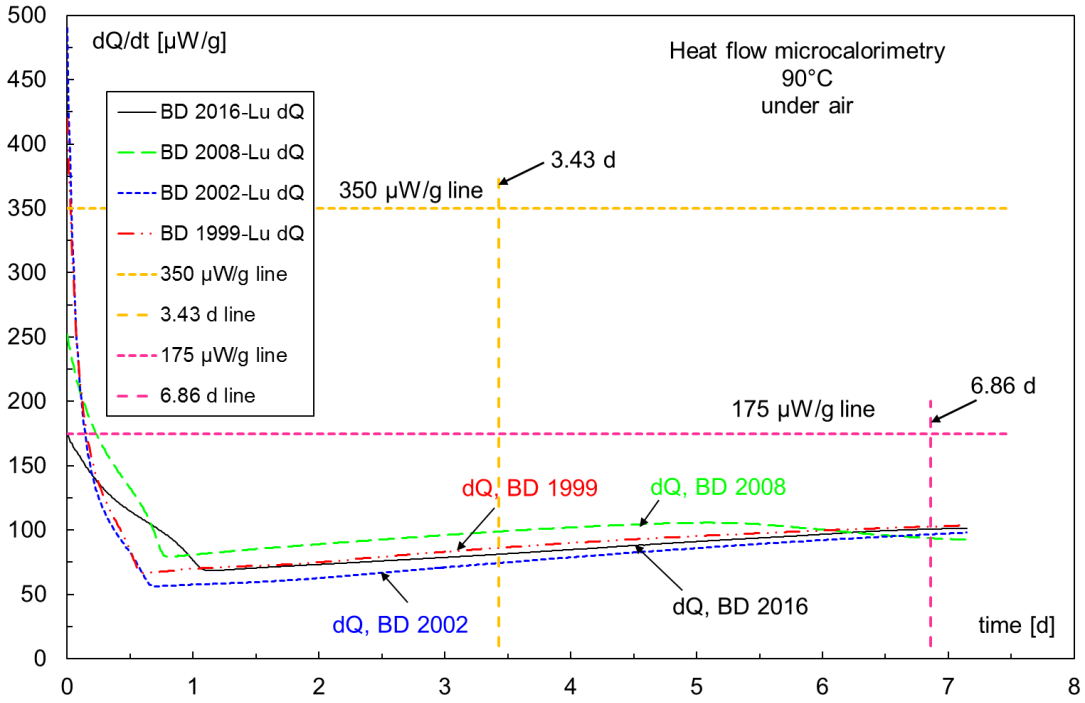

Figure 20-21: Heat generation rate dQ/dt of the four Brazilian db RP, determined at 90°C under air in steel ampoules with glass vial inserts. Shown is also the criterion of STANAG 4582 (HFMC-STANAG). At 90°C the heat generation rate must be below 350 µW/g over 3.43 days, to get the certificate stable over 10 years at 25°C. The samples have such a low heat generation rate that the assessment 20 years at 25°C is possible, because dQ/dt is below 175 µW/g over 6.86 days.

So-named TAM™ II and TAM™ III instruments manufactured by Thermometric AB and Waters Inc., BU TA Instruments, respectively, were used to measure the heat generation rates of the samples. The property for assessment is heat generation rate (HGR) dQ/dt, measured in closed stainless steel ampoules with inserted glass vials to prevent direct contact between steel and the sample. The atmosphere was in one series enclosed air and in another series it was argon, applied via a glove box. From heat generation rate dQ/dt the heat generation Q is obtained by integration over time. The evaluation of the results is done according to the guidelines of the STANAG 4582. The worked out measurement plan allows to choose some measurement temperature in the range 60°C to 100°C and the corresponding measurement times are given. During these measurement times the heat generation rate should not exceed a limit value in order to be assessed chemical stable over 10 years at 25°C. At a measurement temperature of 90°C this limit value is 350 µW/g over a test time of 3.43 days. One can apply the data also for longer predicted time periods. The one has to measure longer. But in order to keep the evolved heat to the same level, the assessment limit must be reduced. When measuring the double test time then the limit value must be half of 350 µW/g. If

the criterion is fulfilled the predicted time period of stability will be 20 years at 25°C. Such an evaluation was done with the four db RP DBRPxxxx and is shown in Figure 21.

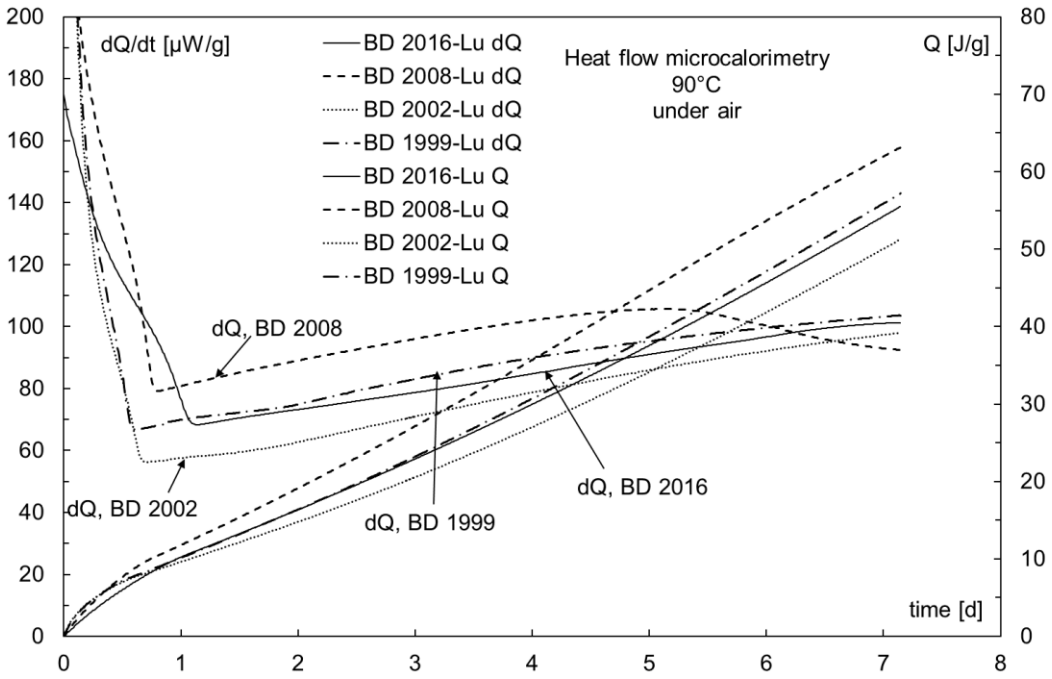

Figure 20-22: Heat generation rate dQ/dt and heat generation Q of the four Brazilian db RP, determined at 90°C under air in steel ampoules with glass vial inserts.

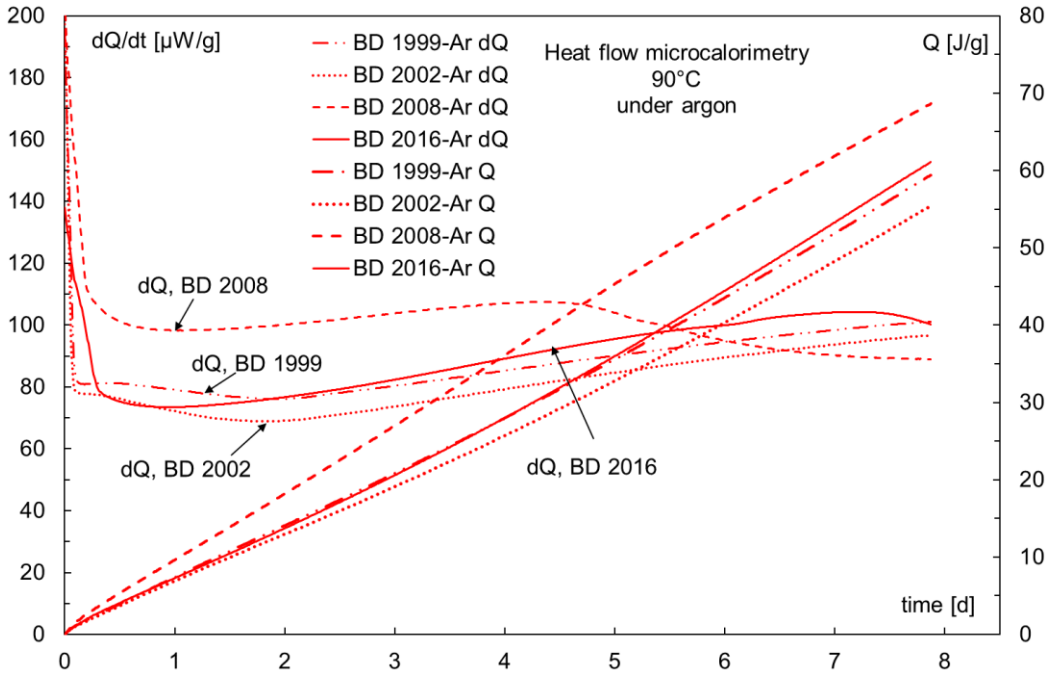

Figure 20-23: Heat generation rate dQ/dt and heat generation Q of the four Brazilian db RP, determined at 90°C under argon in steel ampoules with glass vial inserts.

The Figures 22 and 23 show the measurements under enclosed air and under argon. The main difference can be seen in HGR at the very beginning of the measurements. Under argon, the start of the equilibrated curves is near the time origin. Under air, there is a significant reaction part by the involved oxygen for half

a day. After consumption of oxygen, the curves reach their 'normal' level. As a whole the evolved heat is not much different between these two sets of measurements.

In Figure 24 the adiabatic self heat rates of six db RP can be seen. More or less, they coincide. Mean at higher temperatures this type of propellants decompose in the same way and the slow cook-off behaviour should be quite similar. The data were obtained by an Accelerating Rate Calorimeter (ARC™) of type ES-ARC™ (enhanced system ARC™) from company THT (Thermal Hazard Technology) 1 North House, Bond Avenue, Bletchley, MK1 1SW, England. In order to compare the results the so called thermal inertia and the ϕ-factor should be quite similar [19]. The measurements are performed in spherical titanium cells with one inch in diameter. The factors were in the range 5.85 to 6.12, the sample amounts were 369 mg to 396 mg.

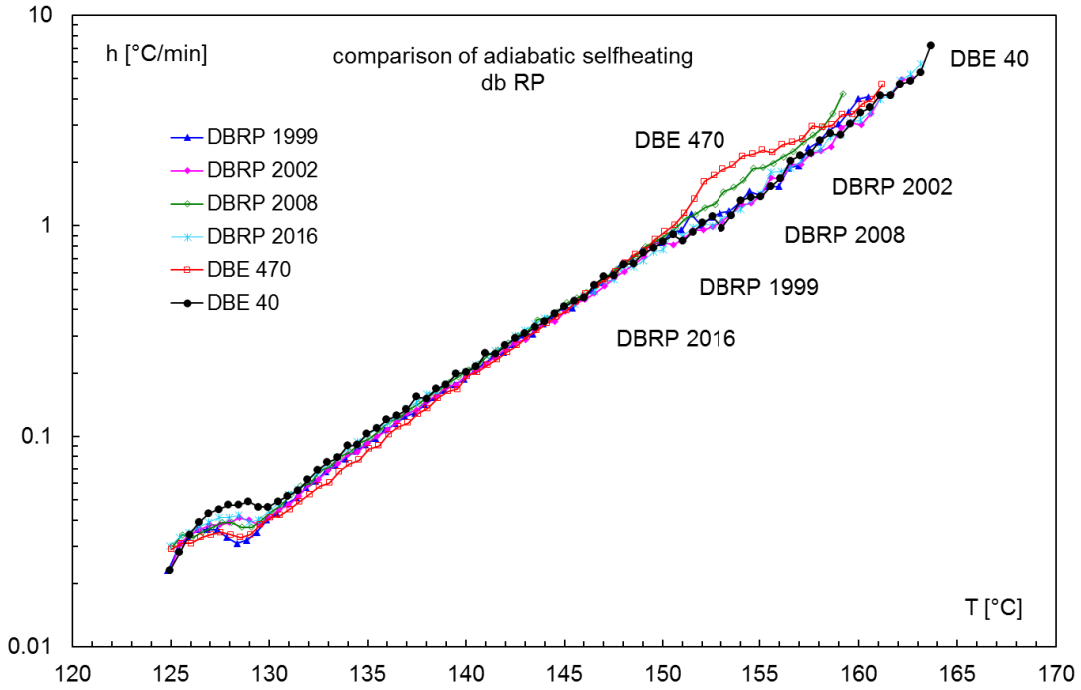

Figure 20-24: Adiabatic selfheating determined by ARCTM (Accelerating Rate Calorimeter) of six db RP. At higher temperature, the decomposition reaction is the same for all db RP. This means the slow cook-off behaviour is the same.

8.0 INFLUENCE OF USED STABILIZER IN DB RP ON GAS GENERATION

From the already discussed db RP also gas generation(GG) was followed at 85°C over time periods of up 44 days. The apparatus used was the P-VST (Pressure Vacuum Stability Tester) of company OZM Research, Blížnovice 32, 538 62 Hrochův Týnec, Czech Republic, called STABIL VI®.

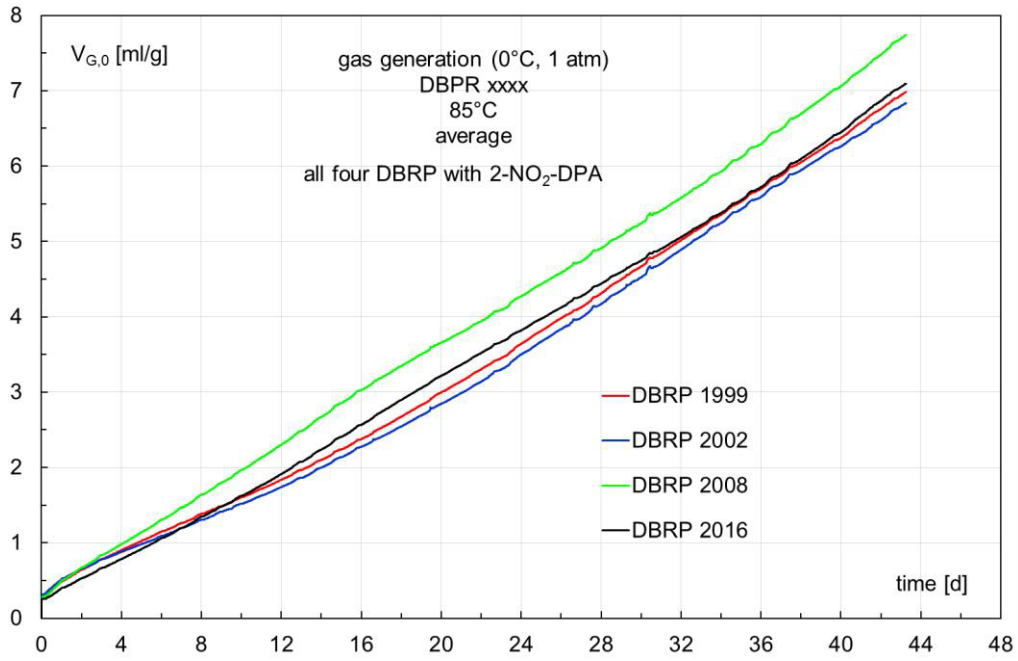

Figure 20-25: Normalized gas generation (calculated for 0°C and 1 atm) of the four Brazilian db RP determined from gas generation at 85°C converted to standardized gas generation.

The data of gas generation as generated gas volume, calculated to standard condition (0°C, 1 atm) for the four db RP DBRPxxxx are shown in Figure 25. The generated gas volume increase nearly linearly at 85°C in this time range. DBRP2008 shows a bit higher GG as the others. This slightly lesser stability was also found with heat generation rate and mass loss for this propellant sample.

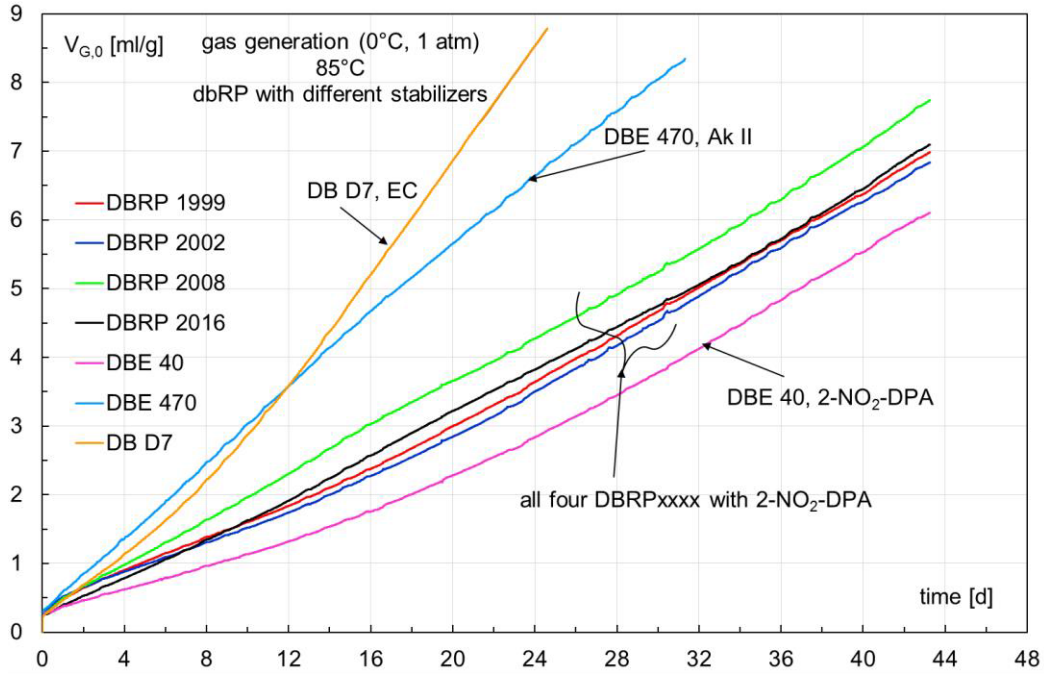

Figure 20-26: Comparison of standardized gas generation (GG) (calculated for 0°C and 1 atm) of db RP, which are differently stabilized. The group stabilized with 2-NO2-DPA show the lowest GG The AK II stabilized propellant shows much higher GG. But the GG of a EC (ethyl centralite or Centralit I) stabilized db RP has the highest rate and is highest of all.

In Figure 26 also the DBE 470 and DBE 40 propellants are included as well as db RP D7, which is stabilized with ethyl centralite (EC). There are significant difference in the rate of gas generation. The lowest rate show the propellants stabilized with 2-NO_2-DPA, then the propellant with Ak II follows. The highest gas generation rate has the propellant with EC as stabilizer. This has consequences on the use of the propellants. Especially in motors with medium diameters, 50 to 100 mm, this gas generation can be critical in the 'internal' pressure by these gases cause fissures in the material. This may disturb severely the burning behaviour of the motors. Therefore, only 2-NO_2-DPA should be used as stabilizer in double base rocket propellants.

9.0 DYNAMIC MECHANICAL ANALYSIS ON DB RP

The DMA method is very useful to determine the glass-rubber transition of elastomers and other polymeric systems forming a rubbery state. The method was extensively used with HTPB bonded propellants and other systems, for example [20, 21]. The measurements were carried out with a DMA instrument of type ARES™ (Advanced Rheometric Expansion System) manufactured from the former rheological group of Rheometric Scientific, Inc. (now belonging to Waters, Inc., BU TA Instruments). The following quantities were determined: storage shear modulus G', loss shear modulus G'', loss factor tanδ = G''/G' as well as the phase angle δ and the torque. Measurements were performed from -110°C to +80°C, with step wise heating up by 1°C/min and soak (equilibration) time of 40s. At each temperature step the specimens were tested after equilibration at four sinusoidal deformation frequencies, 0.1; 1; 10; 30 Hz.

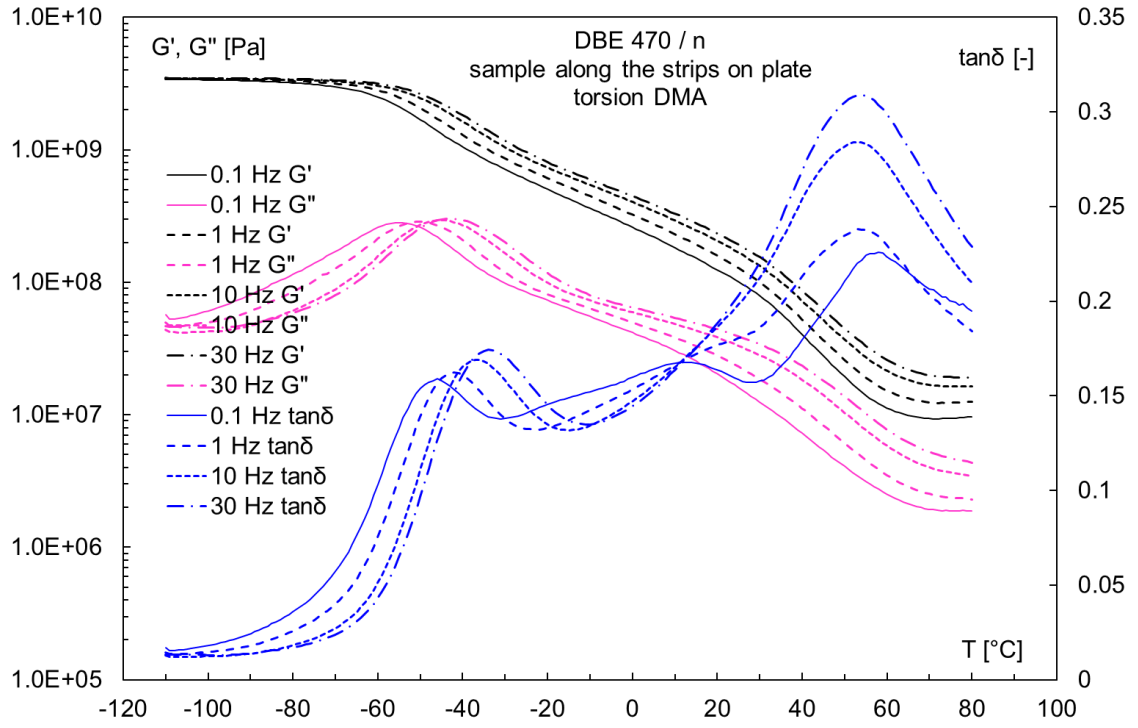

Figure 20-27: Typical DMA results of db RP, here obtained with DBE 470, with DMA in torsion and sinusoidal deformation frequencies between 0.1 and 30 Hz. Sample taken from a plate with rolling stripes, sample cut out along the stripes.

The Figure 27 shows an overview on the measurement with db RP DBE 470. The storage shear modulus G', loss shear modulus G'' and the loss factor tanδ are shown. The propellant has a weak glass-rubber transition (GRT) in the temperature range -50 to -30°C (taken from maximum ranges in tanδ, because the maximum of tanδ represents the highest intensity in molecular reorientation inside the material. The GRT is deformation frequency sensitive it is shifted to higher temperatures with increasing frequency. The other

maximum around +50°C to +60°C is not shifting with increasing frequency. This means here the sample weakens. An interesting feature, because it corresponds to this bend in the Arrhenius plots of Figures 4 and 5. The weakening enables higher diffusion rates and the radicals may be caught easier and faster by stabilizers before they have reacted away with NC backbone. Also to note is the significant increase in tanδ in the temperature range of the material weakening. This means at higher frequency loads, for example by mechanical vibrations, the energy uptake by the sample may be unneglectable.

The samples were cut out from plate material, which was rolled. By this process, it showed stipes on the surface. Therefore, two sample types were investigated, one cut out along the stripes and one cut out across the stripes. Figure 28 shows the data from the sample cut across. In Figure 29 and Figure 30 the two data sets are compared at two deformation frequencies, 0.1 Hz and 10 Hz. No significant differences are recognizable; the plate material was manufactured homogenously by rolling the plate several times orthogonally.

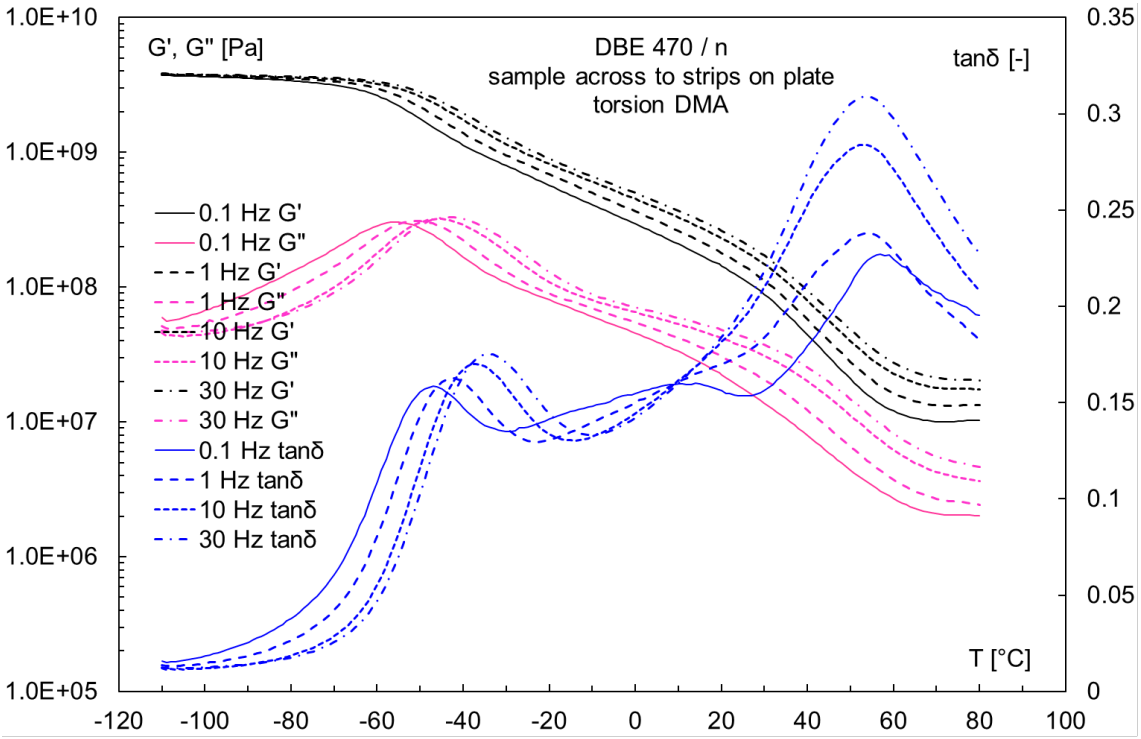

Figure 20-28: Sample DBE 470, DMA in torsion and sinusoidal deformation frequencies between 0.1 and 30 Hz. Sample taken from a plate with rolling stripes, sample cut out across the stripes.

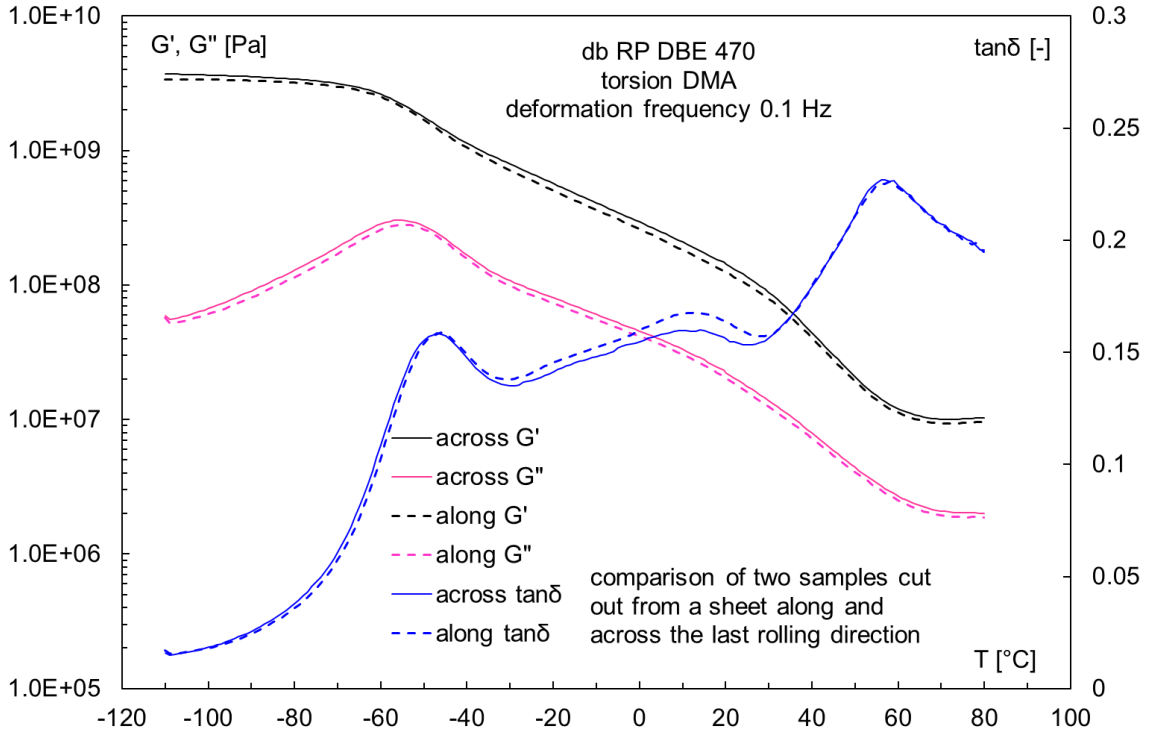

Figure 20-29: Comparison of DBE 470 samples cut out from the plate orthogonally, torsion DMA at 0.1 Hz. There is no significant difference recognizable in the data.

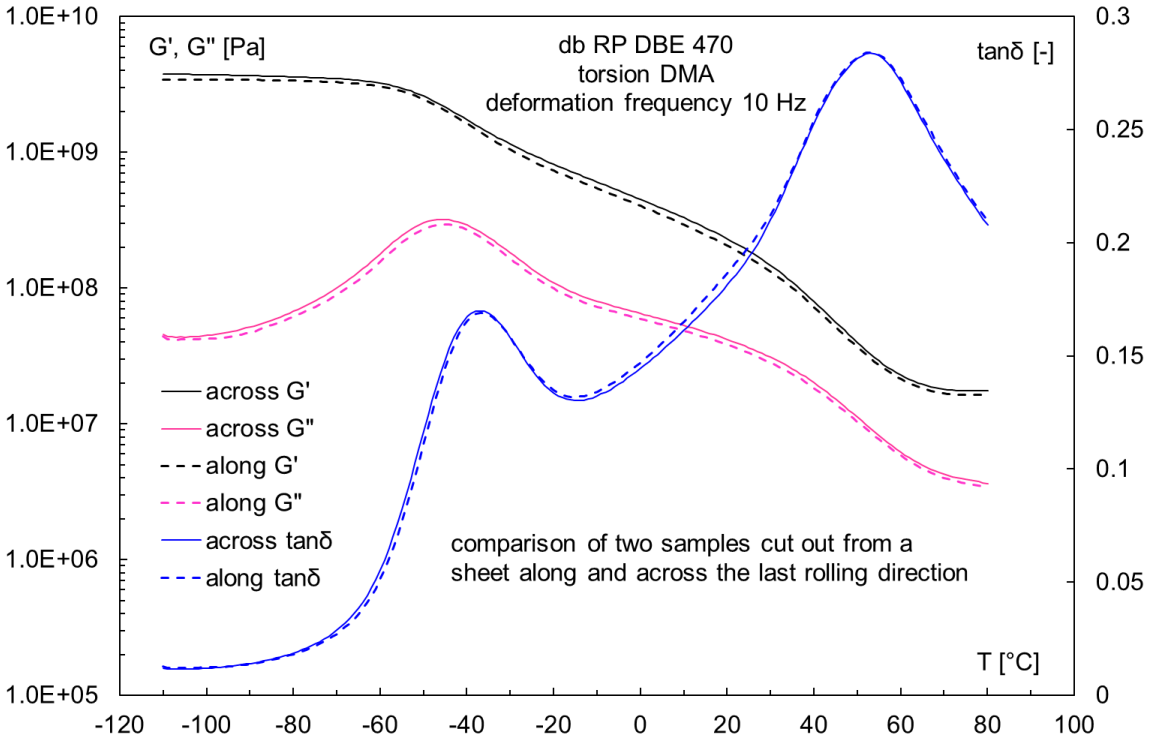

Figure 20-30: Comparison of DBE 470 samples cut out from the plate orthogonally, torsion DMA at 10 Hz. There is no significant difference recognizable in the data.

10.0 MOLAR MASS DISTRIBUTIONS OF SOME DB RP

In the following Figures 31 to 34 several molar mass distribution (MMD) functions of the nitrocellulose in double base rocket propellant formulations are shown. They have been determined by GPC (gel permeation chromatography) with a suitable GPC column set (pore sizes 100 Å, 1000 Å, 100000 Å and 1000000 Å), THF (tetrahydrofuran) as eluent and solvent, UV detector and calibration of the column set by narrowly distributed polystyrene standards, covering the whole separation range of the columns. More experimental and especially chromatogram evaluation details can be found in [22, 23, 24, 25].

Figure 31 compares five db RP formulations. Surprisingly all formulations have very similar MMDs. The demands on the mechanical properties and the gelatinization with nitroglycerine lead to similar nitrocellulose types. But also the ageing behaviour of the propellant formulations seem similar as the following graphs show. In Figure 32 the ageing of NC of DBE 470 can be seen. With ageing the MDDs are shifted to lower molar mass values because of chain splitting of the NC polymer molecules. The ageing was done in HFMC closed ampoules during measurement of the heat generation rate of the propellants. Under air and under argon. It seems that the atmosphere does not have a clear influence on the molar mass degradation of NC. But the reason may be the relatively small amount of available oxygen in the ampoules with about 2 ml free volume and 4 ml total volume. Also the formulation BD-2008 and BD 2016 show behaviour analogous to DBE 470.

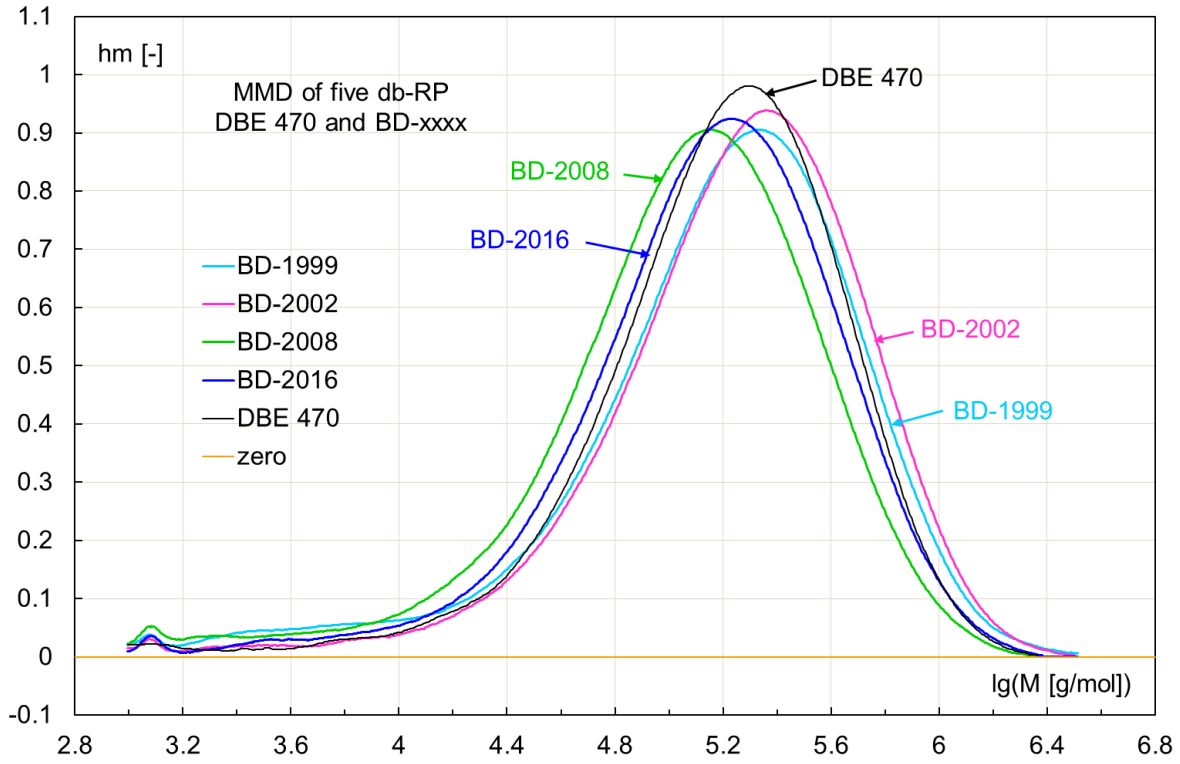

Figure 20-31: Comparison of the molar mass distributions (MMD) of five double base rocket propellant formulations. All five MMD are similar and this in spite of the age of some formulations.

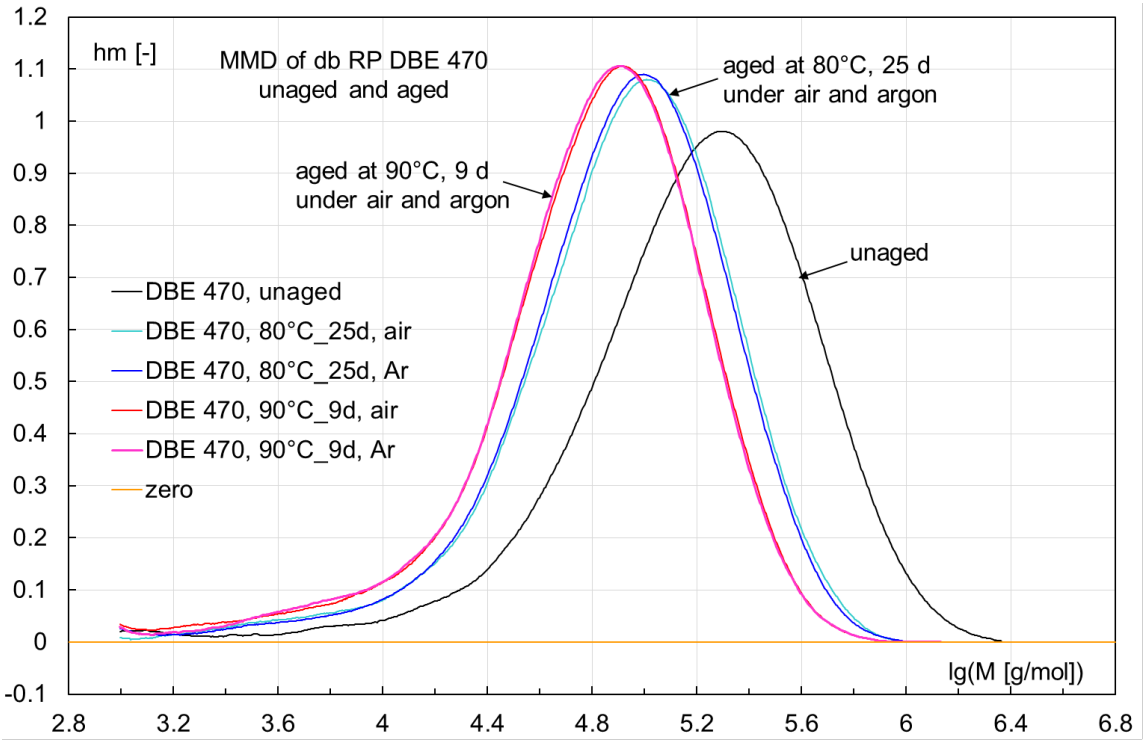

Figure 20-32: Comparison of the molar mass distributions (MMD) of unaged and aged samples of DBE 470. Samples aged in closed ampoules under air and under argon, after the HFMC measurements of the samples. By ageing the MMD is shifted to lower molar masses. It seems that in closed ampoules the ageing is not much influenced by residual air.

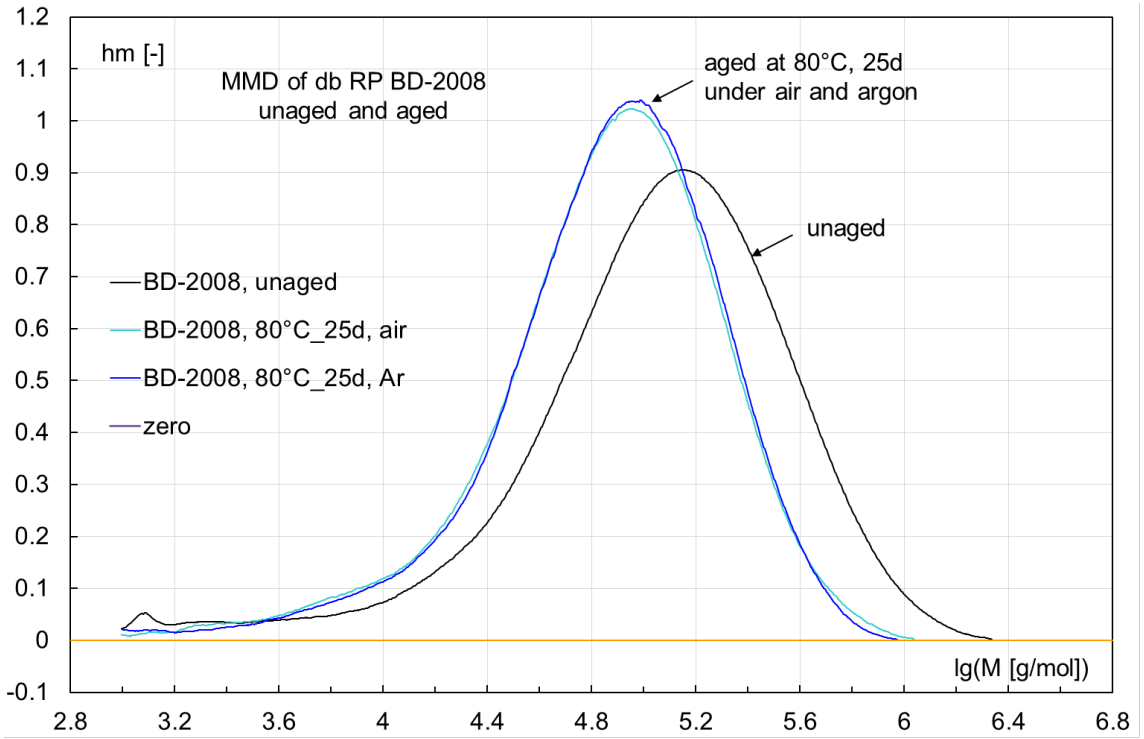

Figure 20-33: Comparison of the molar mass distributions (MMD) of unaged and aged samples of BD-2008. Samples aged in closed ampoules under air and under argon, after the HFMC measurements of the samples. By ageing the MMD is shifted to lower molar masses. It seems that in closed ampoules the ageing is not much influenced by residual air.

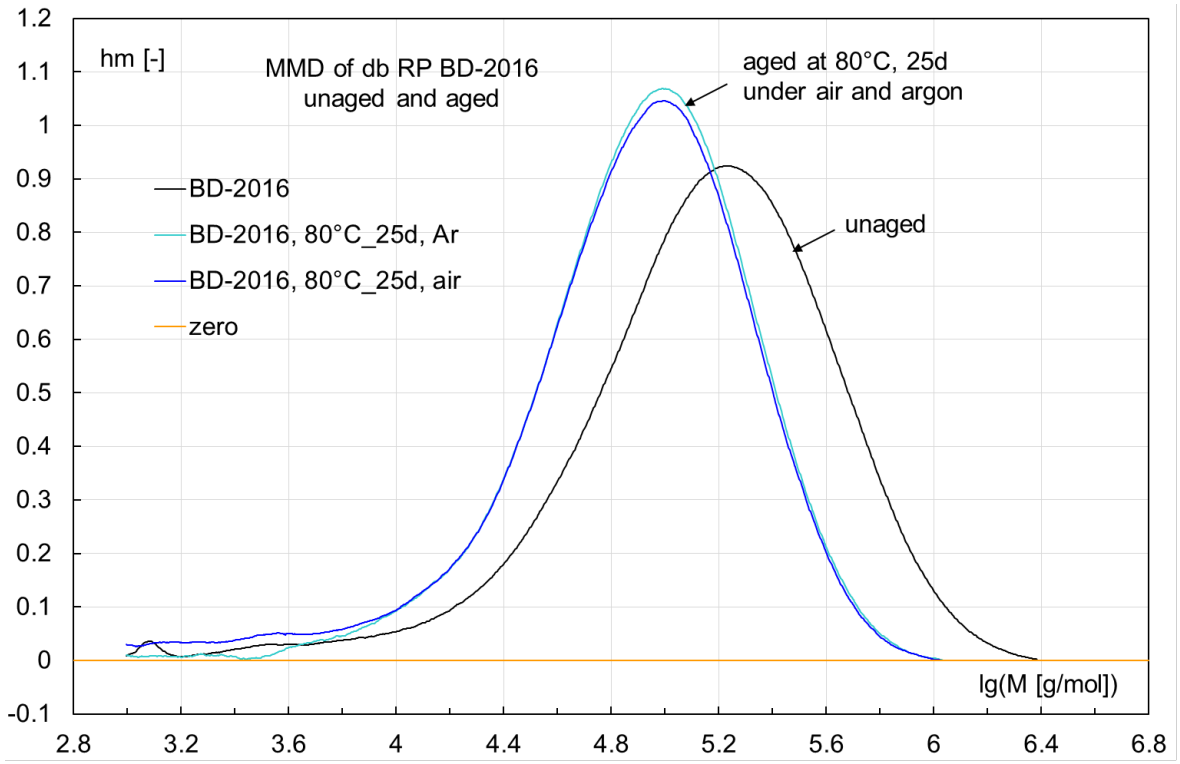

Figure 20-34: Comparison of the molar mass distributions (MMD) of unaged and aged samples of BD-2016. Samples aged in closed ampoules under air and under argon, after the HFMC measurements of the samples. By ageing the MMD is shifted to lower molar masses. It seems that in closed ampoules the ageing is not much influenced by residual air.

Table 20-8: Characterizing data of the molar mass distributions.

formulation	Mn [kg/mol]	Mw [kg/mol]	Mz [kg/mol]	Mp [kg/mol	D = Mw/Mn
DBE 470, unaged	60.43	240.8	463.2	208.9	3.99
DBE 470, 80°C, 25d, Ar	39.80	116.7	228.1	100.8	2.93
DBE 470, 80°C, 25d, air	41.39	120.5	211.3	106.4	2.91
DBE 470, 90°C, 9d, Ar	32.31	92.68	162.5	82.17	2.87
DBE 470, 90°C, 9d, air	30.55	93.61	163.8	84.07	3.06
BD-2008, unaged	36.87	191.3	414.8	146.7	5.19
BD-2008, 80°C, 25d, Ar	35.75	110.4	201.2	98.43	3.09
BD-2008, 80°C, 25d, air	34.80	111.2	216.0	91.57	3.20
BD-2016, unaged	52.31	227.2	474.4	175.5	4.34
BD-2016, 80°C, 25d, Ar	46.61	119.1	214.6	102.0	2.56
BD-2016, 80°C, 25d, air	32.37	114.9	211.1	100.3	3.55

11.0 NEW STABILIZERS FOR FORMULATIONS BASED ON NITRATE ESTER COMPOUNDS – DEMANDS AND WAY OF ASSESSMENT

The propagated advantage of all stabilizers offered as new during the last years emphasize their 'greeness', means they contain not such nitrogen groups, which may form N-nitroso compounds. From such N-nitroso compounds, the ones with N-alkyl side groups are the most dangerous ones, because they can produce cancer via the alkylation of DNA and RNA. Therefore ethylcentralite (Centralite I) is on the list for unwanted substances, also the stabilizer MNA (N-methyl para nitro-aniline). Much less harmful are DPA, 2-nitro-DPA and Akardite II. But 'greenness' alone cannot be the only objective. The selected substances must perform the stabilization of the products, means all types of gun propellants and of double base rocket propellants. The reference stabilizers are Akardite II, 2-nitro-diphenylamine (2-NO_2-DPA) and still DPA itself. The usual way to prove the effectiveness of a selected substance as stabilizer uses test formulations, which must be manufactured and the stabilization quality tested in comparison to the standard stabilizers. The question is, which tests must be performed. The testing must be thoroughly, scrupulous and even nit-picking in order to avoid unwanted surprises during later use of the new stabilizers. For easy use, the substances should be analysable with HPLC and easily extractable from the formulations. Reaction products, which are formed by reaction with NO / NO_2 split-off from nitrate ester groups, must be identified and also the possible consecutive products. To be complete, toxicity investigations must be performed from the start substances and the consecutive products.

The following tests must be done in order to achieve a complete suitability assessment:

- Ageing series with stabilizer decrease followed by extraction and HPLC analysis at several temperatures including higher and lower temperatures: 60°C, 70°C, 80°C, 90°C;
- Mass loss measurements at several temperatures, to be measured until active stabilizer is consumed;
- Gas generation at several temperatures measured continuously in VST-type experiments; this procedure is not complementary to mass loss, therefore both methods must be applied;
- Heat flow calorimetry at several temperatures over longer time intervals, means at 80°C at least over 20 days; 7 days at 90°C and 60 days at 70°C;
- Investigation in application of typical kinetic models for stabilizer decrease;
- Determination of Arrhenius activation parameters by Friedman-analysis and by model applications;
- Determination of consecutive products;
- Determination of molar mass distribution of NC used in the formulations after an ageing series; comparison of the rates of the decrease of mean molar masses Mn, Mw and Mz;
- Bergmann-Junk or Bergmann-Junk-Siebert testing, in order to get an evaluation of the behaviour at higher load temperatures;
- Autoignition temperature behaviour;
- Cube-crack test with cube edge length of 50mm at 80°C applied over at least 10 days; to be applied for double base rocket propellant formulations; detects formation of flaws by gas production;
- Determination of burning behaviour with strands in Crawford type instrumentation;
- Determination of burning behaviour for gun propellant formulations;
- Slow cook-off behaviour or as an alternative the adiabatic selfheating measured by ARC™ (Accelerated Rate Calorimetry);
- Testing of the selected substances on possible toxicity behaviour for humans, animals and aquatic organisms

12.0 COMPILATION OF TEST AND INVESTIGATION METHODS

Method	Development of RP	In-service surveillance (ISS)	Remarks	Usable non-destructive
Mean molar masses, MMD	yes	can be	NC quality test, by GPC	no
Stabilizer consumption, extraction, HPLC	yes	yes	single temp, acc. AOP 48	no
Stabilizer consumption, extraction, HPLC Ea, Z, predictive	yes	can be	multi temperature test ‘S: exp.+lin’, ‘S: nth order’	no
Mass loss at 90°C, 20 d	yes	can be	chemical stability test, compatibility	no
BJ or BJS, split-off NOx	yes	yes / can be	quantitative stability test	no
Autoignition temperature	yes	yes	Wood metal bath, 5°C/min	no
DSC	yes	can be	crystal. phase changes, onset temp.	no
ARC™	yes / can be	can be	data for slow cook-off simulation	no
Gas generation, 90°C 40h	yes	can be	vacuum stability test (VST), compatibility	no
Continuously recording gas formation	can be	can be	pressure transducer VST	no
Tensile testing	yes	yes (selected)	at several temp., and strain rates	no
Compression testing	yes	yes (selected)	at several temp., and strain rates	no
Temperature cycling	yes	yes	geometric shape stability	yes
Peel test	can be	can be	bonding to layers	no
DMA	yes	can be	glass transition, softening	no
TMA	yes / can be	can be	thermal expansion	no
Heat generation rate (HGR)	yes	yes	chemical stability test, compatibility	no
HGR at several temperatures	can be	can be	probing on thermal explosion	no
Burning behaviour	yes	yes	strand burning	no
chemical composition	yes	yes (in part)		no
Cook-off test	can be	can be	ARC™, as fast method	no
Cube crack test	yes	can be	X-ray of motor	yes
Motor firing	yes	yes	Thrust, burning time	no
Energy content	yes	yes	Heat of explosion	no

MMD molar mass distribution
GPC gel permeation chromatography
HPLC high performance liquid chromatography
ARC accelerating Rate Calorimetry, determines adiabatic self heating
DMA dynamic mechanical analysis
DSC differential scanning calorimetry
TMA thermal mechanical analysis
Ea Arrhenius activation energy
Z Arrhenius pre-factor
VST vacuum stability test
BJ Bergmann-Junk test, determination of split-off NOx
BJS Bergmann-Junk-Siebert test, determination of split-off NOx
HGR heat generation rate determined by HFMC
HFMC heat flow microcalorimetry
Cube crack test: cube edge length 50 mm, test temperature 80°C, stored in a closed AL cylinder, narrowly fitting the cube.
At least during 10 days no flaws should appear inside the cube, determinable x-ray analysis

13.0 SUMMARY AND CONCLUSIONS

Double base rocket propellants (db RP) are an important class of propellants. In spite of their complex decomposition and ageing behaviour, it is not a problem to reach in-service times of 20 years and even more, depending on the thermal loads exerted. There is already a lot of experience on their ageing behaviour and the properties to be selected for in-service time assessment, ageing prediction and so-called structural health monitoring (SHM) is possible on a sound base. The most important aspect with db RP is their chemical stability or better chemical degradation with time. The cause is the complex decomposition behaviour of nitrocellulose (NC). Three main mechanistic decompositions can occur: thermolytic cleavage of the nitre ester group, hydrolytic decomposition of the nitre ester group and hydrolytic cleavage of the NC chain at the 1,4-β-glucosidic bond. All have different activation energies in the range 160 to 170 kJ/mol, 80 to 100 kJ/mol and 60 kJ/mol, respectively. This causes different decomposition activity with changing temperature. The change in measurement properties is not governed by only one activation energy. This effects strongly the prediction of residual in-service time. Mostly a two-mechanistic description of the decomposition of NC-based material is enough and the change in mechanism is in the temperature range 65 to 55 °C. Such a change can be well described with the generalized van't Hoff rule, see [11] for details.

The following properties must be included in a SHM procedure with db RP:

- Stabilizer decrease
- Molar mass decrease of NC
- Tensile properties at break

Helpful is heat flow microcalorimetry for a relatively fast determination of actual chemical stability and for predicting the safe storage period for the next 10 or also 20 years. Gas generation effects on the propellant should be determined according to cube crack test. Already occurred cracks by internal gas generation in the material can be detected by X-ray analysis, which is necessary with motors having medium to large diameters (from web 40 to 50 mm on). The gas generation is controlled by the used stabilizer. Ethyl centralite is the least suitable followed by the somewhat better akardite II. The best one is 2-NO_2-DPA with respect to avoid crack-causing gas generation. Burning rate determination complete the screening.

Tensile properties are affected by the decrease in chain length of the NC. Both strain at break and strass at break decrease proportional to the decrease in mean molar masses Mn or Mw. Also stabilizer decrease and molar mass decrease go in parallel. All four properties are therefore well correlated.

In order to make sound predictions of chemical stability and safe in-service time the stabilizer content is the decisive property. As long as active stabilizer is present, no autocatalytic runaway can occur. Real predictions need the determination of stabilizer decrease as function of time at several isothermal temperatures near in-service situations, means they should be in the range 60°C to 90°C. The next is to apply the best kinetically based descriptions for stabilizer consumption. Mainly two models have proven to give the best description: model 'S: exponential + linear' and model 'S: nth order'. To decide which one is the most adequate with the obtained data, one should perform an analysis based on the information criteria AIC (Akaike Information Criterion) and BIC (Bayes Information Criterion). This gives an objective decision about the models. The same holds to describe the decrease of mean molar mass values. The recently stated and discussed sigmoid stabilizer decrease course is not yet fully confirmed. The presented data up to now give no clear indication for such a behaviour. Anyway, if such a data set is really established, one should use the model developed on the reaction kinetic sound base which is called 'S: bimolecular + NC zero order', which means the stabilizer reaction is bimolecular and the NC decomposition is of zero order.

14.0 ABBREVIATIONS

AIC	Akaike information criterion
Ak II	akardite II, stabilizer
AOP	Allied Ordnance Publication
ARC	Accelerating Rate Calorimetry
BIC	Bayes information criterion
db	double base
DMA	dynamic mechanical analysis
DPA	Diphenylamine, stabilizer
DSC	Dynamic Scanning Calorimetry
EC	ethyl centralite (Centralite I), stabilizer
GPC	gel permeation chromatography (also called SEC, size exclusion chromatography)
HFMC	heat flow microcalorimetry
HGR	heat generation rate
HPLC	high performance liquid chromatography
ML	mass loss
MMD	molar mass distribution, obtained by GPC
Mn	mean molar mass Mn, number average
Mw	mean molar mass Mw, mass (weight) average
Mz	mean molar mass Mz, z average
NC	nitrocellulose
NE	nitrate ester, generally used for substances with CO-NO_2 groups
NG	nitroglycerine
RP	rocket propellant
SHM	structural health monitoring
STANAG	Standardization Agreement
TGA	Thermal Gravimetric Analysis
TMA	thermal mechanical analysis
VST	vacuum stability test

ACKNOWLEDGEMENTS

The company Bayern-Chemie GmbH, Aschau am Inn, is thanked for providing with samples on two double base rocket propellants.

Especially Dr. Giuseppe Tussiwand is thanked in getting the samples.

The Brazilian Army Research Institute, Instituto Militar de Engenharia (IME) in Rio de Janeiro and the Brazilian Navy Research Institute, Instituto de Pesquisas da Marinha (IPqM), in Rio de Janeiro are thanked for providing samples of four double base rocket propellants.

Special thanks go to Major Letivan Gonçalves de Mendonça Filho from IME and to Ms Tétis do Vale Pereira Nascimento Briones, Navy Research Institute (IPqM), now at Directorate of Naval Weapons Systems, Rio de Janeiro.

REFERENCES

[1] M. A. Bohn
Bond dissociation enthalpies of the COeNO2 bonds in nitric acid ester groups and in peroxo-nitrite and peroxo-nitrate groups determined by DFT calculations.
Proceedings 39th International Annual Conference of ICT on Energetic Materials. June 24 to 27, 2008. 71-1 to 71-12. Karlsruhe, Germany. ISSN 0722-4087. Fraunhofer-Institut fuer Chemische Technologie (ICT), D-76318 Pfinztal. Germany.

[2] F. Volk, M. A. Bohn, G. Wunsch
Determination of Chemical and Mechanical Properties of Double Base Propellants during Aging.
Propellants, Explosives, Pyrotechnics 12, 81-87 (1987)

[3] Mohammed Moniruzzaman, John M. Bellerby, Manfred A. Bohn.
Activation energies for the decomposition of nitrate ester groups at the anhydroglucopyranose ring positions C2, C3 and C6 of nitrocellulose using the nitration of a dye as probe.
Polymer Degradation and Stability 102 (2014) 49 – 58.

[4] Manfred A. Bohn, Mohammed Moniruzzaman, John M. Bellerby.
Modelling of the consumption of a dye used to probe the decomposition of nitrocellulose
Proceedings of the 45th International Annual Conference of ICT on 'Energetic Materials (CD-version of the proceedings). Paper 107, pages 107-1 to 107-20. June 24 to 27, 2014, Karlsruhe, Germany. ISSN 0722-4087. Fraunhofer-Institut fuer Chemische Technologie (ICT), D-76318 Pfinztal. Germany.

[5] NATO AOP 48 Edition 2. *Explosives, nitrocellulose based propellants, stability test procedures and requirements using stabilizer depletion*. Brussels, Belgium. NATO Headquarters; October 2008.

[6] M.A. Bohn
Ammunition monitoring in field situations by stabilizer consumption and molar mass decrease as predictive tools.
Proceedings 37th International Annual Conference ICT on Energetic Materials, Paper 25 pages 25-1 to 25-19. June 27 to 30, 2006, Karlsruhe, Germany. ISSN 0722-4087. Fraunhofer-Institut für Chemische Technologie (ICT), D-76318 Pfinztal-Berghausen, Germany.

[7] M. A. Bohn
Prediction of In-Service Time Period of Three Differently Stabilized Single Base Propellants.
Propellants Explos. Pyrotech. 2009, 34, 252 – 266.

[8] M. A. Bohn
Assessment of description quality of models by information theoretical criteria based on Akaike and Schwarz-Bayes applied with stability data of energetic materials.
Proceedings 46th International Annual Conference of ICT on 'Energetic Materials, Paper 6, pages 6-1 to 6-23. June 23 to 26, 2015, Karlsruhe, Germany. ISSN 0722-4087. Fraunhofer-Institut fuer Chemische Technologie (ICT), D-76318 Pfinztal. Germany.

[9] M. A. Bohn, F. Volk.
Aging Behavior of Propellants Investigated by Heat Generation, Stabilizer Consumption, and Molar Mass Degradation.
Propellants, Explosives, Pyrotechnics 17 (1992), pages 171-178.

[10-1] M. A. Bohn
Description of consumption of stabilizers in gun propellants showing pseudo-sigmoid decrease.

Proceedings 44th International Annual Conference of ICT on Energetic Materials, pages 24-1 to 24-40 in CD proceedings (extended and updated version). June 25 to 28, 2013. Karlsruhe, Germany. ISSN 0722-4087. Fraunhofer-Institut fuer Chemische Technologie (ICT), D-76318 Pfinztal. Germany.

[10-2] M. A. Bohn
Problems and faulty uses with the Prout–Tompkins description of autocatalytic reactions and the solutions.
J. Therm. Anal. Calorim. (2014) 116:1061–1072; DOI 10.1007/s10973-013-3509-1.

[11] M. A. Bohn
Prediction of equivalent time-temperature loads for accelerated ageing to simulate preset in-storage ageing and time-temperature profile loads.
Proceedings 40th International Annual Conference of ICT on 'Energetic Materials, Paper 78, pages 78-1 to 78-28. June 23 to 26, 2009, Karlsruhe, Germany. ISSN 0722-4087. Fraunhofer-Institut für Chemische Technologie (ICT), D-76318 Pfinztal-Berghausen. Germany.

[12] Tétis do Vale Pereira Nascimento Briones, Maurício Ferrapontoff Lemos, Marcos Lopes Dias, Letivan Gonçalves de Mendonça Filho, Manfred A. Bohn.
Study on the extension of in-service times of double base rocket propellants used in 70 mm rocket motors.
Proceedings 48th International Annual Conference of ICT on Energetic Materials', June 27 to 30, 2017, Karlsruhe, Germany. ISSN 0722-4087. Fraunhofer-Institut fuer Chemische Technologie (ICT), D-76318 Pfinztal. Germany.

[13] M. A. Bohn
Ageing analysis by mass loss measurements of single base propellants used as gas generants in high thermal load environments.
Proceedings 41th International Annual Conference of ICT on 'Energetic Materials (CD version), Paper 115, pages 115-1 to 115-26. June 29 to July 2, 2010, Karlsruhe, Germany. ISSN 0722-4087. Fraunhofer-Institut für Chemische Technologie (ICT), D-76318 Pfinztal. Germany.

[14] Bohn, M.A.
The characterization of time-temperature profiles by reaction kinetic determined mean temperature values.
Proceedings 42nd International Annual Conference of ICT on 'Energetic Materials, June 28 to July 1, 2011. Paper 51, pages 51-1 to 51-26. Karlsruhe, Germany. ISSN 0722-4087. Fraunhofer-Institut für Chemische Technologie (ICT), D-76318 Pfinztal. Germany. Version CD-Proceedings.

[15] Moritz Heil, Kerstin Wimmer, Manfred A. Bohn
Characterization of different gun propellants by long term mass loss.
Proceedings 47th International Annual Conference of ICT on Energetic Materials, paper 37, pages 37-1 to 37-16. June 28 to July 1, 2016, Karlsruhe, Germany. ISSN 0722-4087. Fraunhofer-Institut fuer Chemische Technologie (ICT), D-76318 Pfinztal. Germany.

[16] NATO Standardization Agreement (NATO STANAG) 4582 '*Explosives, Nitrocellulose Based Propellants, Stability Test Procedure and Requirements Using Heat Flow Calorimetry'*
Military Agency for Standardization, NATO Headquarters, Brussels, Belgium.

[17] Ticmanis U., Wilker S., Pantel G., Kaiser M., Guillaume P., Balès C., van der Meer N.
Principles of a STANAG for the estimation of the chemical stability of propellants by heat flow calorimetry.
Proceed. 31st International Annual Conference of ICT on Energetic Materials. Paper 2, pages 2-1 to 2-20. June 27 to 30, 2000, Karlsruhe, Germany. ISSN 0722-4087. Fraunhofer-Institut für Chemische Technolo-

gie (ICT), D-76318 Pfinztal-Berghausen, Germany.

[18] M. A. Bohn
Safety analysis of a single base propellant for automotive use with heat generation rate and prediction of in-service times.
Proceedings 41th International Annual Conference of ICT on 'Energetic Materials (CD version), Paper 116, pages 116-1 to 116-42. June 29 to July 2, 2010, Karlsruhe, Germany. ISSN 0722-4087. Fraunhofer-Institut für Chemische Technologie (ICT), D-76318 Pfinztal-Berghausen.

[19] Manfred A. Bohn, Heike Pontius
Thermal Behaviour of Energetic Materials in Adiabatic Selfheating Determined by ARC™.
Proceedings (CD-version) 43rd International Annual Conference of ICT on Energetic Materials, paper 57, pages 57-1 to 57-40. June 26 to 29, 2012, Karlsruhe, Germany. ISSN 0722-4087. Fraunhofer-Institut fuer Chemische Technologie (ICT), D-76318 Pfinztal. Germany.

[20] Manfred A. Bohn, Günter Mußbach, Sara Cerri.
Influences on the loss factor of elastomer binders and its modelling.
Proceedings 43rd International Annual Conference of ICT on Energetic Materials, paper 60, pages 60-1 to 60-43. June 26 to 29, 2012, Karlsruhe, Germany. ISSN 0722-4087. Fraunhofer-Institut fuer Chemische Technologie (ICT), D-76318 Pfinztal. Germany.

[21] Sara Cerri, Manfred A. Bohn, Klaus Menke, Luciano Galfetti.
Ageing of HTPB/Al/AP rocket propellant formulations investigated by DMA measurements.
Propellants Explosives Pyrotechnics 38, 190 - 198 (2013).

[22] Manfred A. Bohn, Norbert Eisenreich.
Kinetic modelling of the change of molar mass distribution function of nitrocellulose during ageing
Proceed. (CD-version) 41th International Annual Conference of ICT on Energetic Materials. Paper 86, pages 86-1 to 86-24. June 29 to July 2, 2010, Karlsruhe, Germany. ISSN 0722-4087. Fraunhofer-Institut für Chemische Technologie (ICT), D-76318 Pfinztal-Berghausen, Germany.

[23] Manfred A. Bohn, Manuela Dörich, Heike Pontius.
Gel permeation chromatography of nitrocellulose (NC) and NC containing substances. II. Remarks on calibration, molar mass distributions and mean molar masses.
Proceed. 39th International Annual Conference of ICT on Energetic Materials. Paper 70, pages 70-1 to 70-22. June 24 to 27, 2008, Karlsruhe, Germany. ISSN 0722-4087. Fraunhofer-Institut für Chemische Technologie (ICT), D-76318 Pfinztal-Berghausen, Germany.

[24] Heike Pontius, Manuela Dörich, Manfred A. Bohn
Gel permeation chromatography of nitrocellulose (NC) and NC containing substances. I. Parameter study for preparation of NC solutions and chromatogram evaluation.
Proceed. 39th International Annual Conference of ICT on Energetic Materials. Paper 69, pages 69-1 to 69-15. June 24 to 27, 2008, Karlsruhe, Germany. ISSN 0722-4087. Fraunhofer-Institut für Chemische Technologie (ICT), D-76318 Pfinztal-Berghausen, Germany.

[25] Heike Pontius, Manuela Dörich, Manfred A. Bohn
Gel permeation chromatography of nitrocellulose (NC) and NC containing substances. III. Recent results from a continued parameter study on the GPC of NC samples.
Proceed. 40th International Annual Conference of ICT on Energetic Materials. Paper 80, pages 80-1 to 80-12. June 23 to 26, 2009, Karlsruhe, Germany. ISSN 0722-4087.Fraunhofer-Institut für Chemische Technologie (ICT), D-76318 Pfinztal-Berghausen. Germany.